Interfacial and Nanoscale Science Facility

The Interfacial & Nanoscale Science Facility (INSF) is a world-class resource for scientific expertise and instrumentation focused on the study of interfacial phenomena and nanoscience and technology. This section summarizes the capabilities available in the INSF, along with research programs associated with facility users. Activities in the facility address national needs in environmental restoration, waste management, pollution prevention, energy production and storage, and national and homeland security through research that specializes in preparation, characterization, and reactivity of surfaces and interfaces. The range of scientific expertise and instrumentation within the facility provides a unique environment for research in areas such as nanoscience and nanotechnology; interfacial catalytic chemistry; designed oxide interfaces, including environmental aerosol and mineral interfaces; materials and chemoselective interfaces; and areas within microanalytical science, such as chemical sensing and nanobiotechnology.

The INSF and its scientific staff provide a broad range of instrumentation, laboratory capabilities, and expertise. Instrumentation is available for chemical synthesis, analytical chemistry, separations, electrochemistry, thin-film deposition, catalytic reactors, ion-beam processing, and microfabrication. Capabilities include an accelerator facility for material modification and analysis using ion beams along with interface characterization; scanning probe microscopies; electron microscopy and x-ray analysis; spectroelectrochemistry; high-spatial/energy resolution surface analysis; catalyst preparation, characterization, and reaction engineering; a fully equipped clean room for microfabrication, microanalytical systems development, and testing laboratories; inorganic, organic, polymer, and biochemical synthesis and characterization facilities; a full complement of thin-film deposition and characterization facilities; and fully equipped analytical support laboratories. The combination of surface and interface characterization techniques that provide high spatial, depth, and energy resolution for a broad array of methods is unmatched anywhere in the world. Many systems are coupled directly to film growth chambers, and samples can be moved among 16 different systems under controlled environments without exposure to air.

Instrumentation & Capabilities

- Thin-film deposition
- Surface analysis suite
- Electron microscopy suite
- Scanning probe microscopy
- Ion-beam processing and analysis
- Nanobiotechnology capabilities
- Surface Science and Catalysis Laboratory
- Catalytic reactors
- X-ray diffraction laboratory
- Microfabrication
- Chemical and biological sensing
- Other analytical and characterization laboratories

Staff assigned to the INSF perform innovative research in the areas of surface and interfacial chemistry, advanced materials synthesis and characterization, and microanalytical science. Our activities emphasize research relevant to the four U.S. Department of Energy (DOE) mission areas—science, energy resources, environmental quality, and national security—and to operation of a world-class user facility that supports the DOE science mission. Our staff also plays a major role in the continued success of the W.R. Wiley Environmental Molecular Sciences Laboratory (EMSL) by providing support, training, and collaboration to onsite

users. Over the past seven years, research activities in the INSF have focused on four major thrust areas: 1) films and interphases, 2) surface chemistry and catalysis, 3) material interfaces, and 4) microsensors, microfluidics, and new biotechnologies. Staff assigned to the INSF continue to focus their efforts in these four areas with research on the following topics:

- *Oxide and Mineral Films and Surfaces*. Structural and chemical properties of model single-crystal oxide and complex mineral surfaces.
- *Electronic and Catalytic Materials*. High dielectric materials, magnetic oxide semiconductors, and oxide catalysts.
- *Nanoscale Materials*. Oxide quantum dots and nanofilms of magnetic and oxygen ion-conducting oxides, buried nanoclusters in oxides.
- *Interfacial Properties and Reactivity*. Reactions at oxide and mineral interfaces and the structural and chemical properties.
- *Microanalytical Separations and Sensing*. Development of new microanalytical and sensing principles, tools, and testing.
- *Nanobiotechnology*. Single-enzyme nanoparticles, enzymes in nanostructured matrices; understanding the dynamics of these materials.
- *Environmental Studies*. Waste separations, structural and chemical stability of waste forms under different radiation and chemical environment, atmospheric aerosols.
- *Analysis and Characterization*. Fully equipped analytical laboratories and characterization facilities.

Films and Interphases. The physical and chemical properties of the region between single phases of a material (i.e., the interphase) have a major influence on many characteristics of the material, including stability, electronic properties, atomic and ionic transport, and chemical reactivity. Research programs include the synthesis of thin films and nanostructured materials, both of which contain a high concentration of interphase regions. Research activities also involve studies of solid/solid, solid/liquid, and solid/gas (or vacuum) interphase regions. Although most studies are focused on inorganic materials and interphases, organic and biological systems are becoming an increasingly large part of our work.

Surface Chemistry and Catalysis. Basic research is carried out with the most simple, well-defined, environmentally relevant crystallographic structures (e.g., mineral carbonates, metal oxides) for which molecular theory and spectroscopy are immediately applicable. The work then progresses to materials with more complex structures, such as iron and titanium oxides with substitutional impurities. For example, fundamental studies of the oxygen storage and release properties of pure and zirconium-doped ceria single-crystal thin films are aimed at understanding how these "oxygen storage materials" perform in an automobile exhaust system catalytic converter. In addition to fundamental surface chemistry research, we are developing materials and reactor designs for a number of heterogeneous catalytic processes. One study involves synthesizing, characterizing, and testing a group of novel, mesoporous, silica-supported, solid-acid catalysts for use in petroleum-refining processes.

Material Interfaces. Studies are being conducted in several areas: solid/solid interfaces in a wide variety of materials, radiation effects in materials, fundamental defect properties and

interactions, atomic and ionic transport, and aerosol characterization. Many of the studies on solid/solid interfaces involve 1) characterization of interfaces between thin films and substrates, between ion-beam-modified surfaces and the original substrate, or between nanoclusters and host matrices; 2) segregation or diffusion of point defects, impurities, dopants, or gas atoms to or from such interfaces; 3) transport of hydrogen, oxygen, or other gases across such interfaces; 4) formation or destruction of such interfaces from radiation damage processes; and 5) stability of interfaces under a wide range of environmental conditions. Studies on radiation effects include experimental research on materials for immobilization of nuclear waste and plutonium, as well as materials for next-generation nuclear power production, wide-band-gap semiconductors, and multiscale computer simulations of damage production processes, defect diffusion, and microstructure evolution. Studies on atomic and ionic transport include ion exchange processes in nuclear waste glasses, hydrogen storage and transport in materials, and oxygen transport in fast ion conductors.

Microsensors, Microfluids, and Nanobiotechnology. This research includes four primary thrust areas: 1) array-based vapor sensors, 2) nanoscience, 3) bioanalytical microfluidics, and 4) radioanalytical microfluidics. Key areas of science in array-based vapor-sensing include rational design, development, and synthesis of polymeric-sensing materials, linear free-energy models for vapor/polymer interactions, organic thin films, photo-patterning methods for sensor materials, integrated sensor systems, and multivariate data analyses. The nanoscience area includes development of monolayer-protected gold nanoparticles for use on sorptive sensing films, single-enzyme nanoparticles as a new nanostructure for enzyme stabilization, and multi-functional nanoparticle assemblies for biodetection. The latter two areas represent a new thrust in nanobiotechnology, and a laboratory within EMSL has been established for synthesizing enzyme nanostructures and studying enzyme kinetics and enzymes in nanostructured matrices. Experimental research in bioanalytical microfluidics and radioanalytical microfluidics is now located primarily in other facilities, but close scientific ties with EMSL are maintained.

Capabilities

Thin-Film Deposition. Thin-film deposition capabilities include oxygen plasma-assisted molecular beam epitaxy (MBE) systems (Figure 1), a metal organic chemical vapor deposition system (MOCVD), and a sputter deposition system. The MBE systems consist of growth chambers connected to surface characterization chambers through sample transfer lines. The growth chambers have various electron beam and effusion cell sources along with reflection high-energy electron diffraction and quartz crystal oscillators to monitor the growth. The surface characterization chambers are equipped with several surface-science capabilities including x-ray photoelectron spectroscopy (XPS)/diffraction, Auger electron spectroscopy (AES) low-energy electron diffraction (LEED), and atomic force microscopy/scanning tunneling microscopy (AFM/STM). The MOCVD system is specially designed for epitaxial growth of oxide thin films. The system comprises a rotating

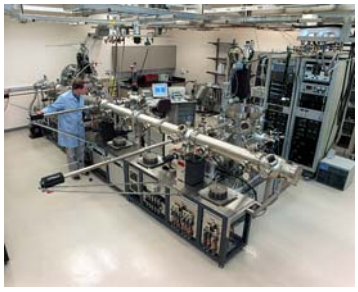

Figure 1. Oxygen plasma-assisted MBE system.

disk reactor, two metal organic source delivery systems (bubbler vapor-phase and direct liquid source-injection), an oxygen microwave plasma unit, a spectroscopic ellipsometer, and a Fourier transform infrared (FTIR) spectrometer. The system is capable of growing uniform (in both thickness and composition) oxide thin films with abrupt interfaces. The sputter deposition system consists of radio frequency and direct current sputtering sources.

Surface Analysis Suite. The surface analysis suite consists of a Physical Electronics Instruments (PHI) Quantum 2000 high-resolution, x-ray photoelectron spectrometer (Figure 2), a Kratos Axis multi-technique surface analysis system (SAS), a PHI Model T2100 time-of-flight secondary ion mass spectrometer (TOF-SIMS), and a PHI Model 680 AES/scanning Auger microprobe. The Quantum 2000 XPS system is unique in that it uses a focused monochromatic Al K α x-ray beam that can be varied in size from as small as 10 μm in diameter to approximately 200 μm. The TOF-SIMS system uses a pulsed and focused ion source and TOF analyzer to obtain high spatial- and mass-resolution data from a specimen surface. The multi-technique SAS enables surfaces to be probed with a variety of complementary analysis methods, and contains electron imaging, electron spectroscopy, and both primary and secondary ion-scattering capabilities. The Model 680 auger electron spectrometer (AES)/scanning Auger microprobe is based on a field-emission electron source and a cylindrical mirror analyzer. The electron beam size can be focused as low as 10 nm at 20 kV, although somewhat larger beams are typically used to collect AES data. Instrument features and capabilities include beam rastering, scanning electron microscope (SEM) imaging, mapping, specimen cleaning and depth profiling using a sputter gun, and sample rotation to allow "Zalar" rotation during sputtering. The system also is configured with an x-ray detector for near-surface analysis in combination with AES surface analysis.

Figure 2. X-ray photoelectron spectrometer.

Electron Microscopy Suite. The electron microscopy suite consists of a LEO 982 field-emission scanning electron microscope (FESEM), a high-resolution transmission electron microscope (TEM) (Figure 3), and another cryo-TEM dedicated for biological work (Cryo TEM). The FESEM is an ultrahigh-performance SEM with a resolution of 1 nm at 30 kV and 4 nm at 1.0 kV. It has a large specimen chamber equipped with multiple detectors, a below-lens secondary electron detector, an in-lens secondary electron detector, a backscatter electron detector, an energy-dispersive x-ray detector, and an electron backscatter diffraction detector. The JEOL 2010 is a high-resolution TEM with a spatial resolution of 0.194 nm. This instrument has a medium acceleration voltage of 200 kV, a high-brightness electron source, digital image recording, a computer-controlled sample goniometer, and a geometrically optimized x-ray detector. It has a wide range of illumination lens conditions:

Figure 3. High-resolution TEM.

TEM mode, energy-dispersive spectroscopy mode, nanometer beam electron diffraction, and convergent beam electron diffraction. The TEM is post-column attached with a Gatan image filter, giving an optimized energy resolution of approximately 1.2 eV, which allows analysis of light elements by electron energy-loss spectroscopy and elemental mapping in the electron spectroscopic imaging. The Cryo TEM is primarily used for biological imaging and tomography. The spatial resolution of the instrument is about 0.45 nm, and it has an accelerator voltage in the range of 80 to 120 kV.

Scanning Probe Microscopy. The scanning probe microscopy laboratory has a Digital Instrument Nanoscope IIIa AFM, a Topometrix TMX 1000 Explorer SPM, and an Omicron variable non-contact ultrahigh vacuum (UHV) AFM/STM system with surface-science capabilities including XPS, Auger electron microscopy, plasma cleaning, and deposition. The instrument is capable of operating in both air and liquid environments and in several modes that include contact, tapping, frictional force, phase/frequency, capacitance, and magnetic/electrostatic force. As a real space probe, the instrument can be used to probe surface morphology, defects, and electrostatic, magnetic, dopant concentration, and mechanical properties of conducting and non-conducting materials. The Topometrix TMX 1000 Explorer SPM can be used for both AFM and STM in air and in liquid and is particularly useful for larger samples. This instrument includes both contact and non-contact AFM modes. STM requires an electrically conductive sample and produces images based on the topography and electronic structure of the sample. AFM samples may be insulating or conducting; the image is based on the force between the AFM probe and the sample and is primarily a map of the surface topography. The Omicron variable scanning probe microscope can be used for both STM and AFM under UHV conditions. As a real space probe, this instrument is designed to probe surface structure, defects, and morphology of conducting and non-conducting materials. In addition to STM/AFM, the vacuum system also is equipped with other surface-science capabilities that include LEED, XPS, AES, and oxygen plasma cleaning.

Ion-Beam Processing and Analysis. The accelerator facility (Figure 4) is equipped with capabilities to perform material modification and analysis using high-energy ion beams. The facility has two ion sources, a 3-MeV tandem ion accelerator, injector and analyzing magnets, beam lines, and four end stations. The end station on the +30° beam line is equipped with LEED, AES, XPS, oxygen plasma, and sputter cleaning sources and effusion cells in addition to the conventional ion-beam capabilities. Ion-beam capabilities include fixed and movable detectors for Rutherford backscattering spectrometry/channeling, nuclear reaction analysis (NRA), and elastic recoil detection analysis (ERDA). This beam line extends through the end station to another end station where experiments can be performed with the beam size of 20 microns or greater. The micro-beam end station is also equipped with capabilities for conventional ion-beam techniques including RBS, NRA, and proton-induced x-ray emission (PIXE). The +15° beam line is equipped with a raster scanner for ion implantation and ion-beam modification of materials, and the end station is equipped with all the conventional ion-beam capabilities. In addition, this beam line is equipped with

Figure 4. Accelerator facility.

heavy ion elastic recoil detection analysis capability for material characterization. The −15° end station is designed to carry out routine analytical work. The NEC RC 43 end station attached to this beam line is equipped with most of the standard ion-beam analytical capabilities including RBS, NRA, PIXE, particle-induced gamma emission, proton elastic scattering analysis, scanning transmission ion microscopy, and ERDA.

Surface Science and Catalysis Laboratory. Three UHV surface chemistry systems designed for studies of the molecular-level chemistry of adsorbates on metal oxide surfaces are available in the Surface Science and Catalysis Laboratory. These systems are equipped with a number of spectroscopic tools to follow changes in adsorbate chemistry, including high-resolution electron energy-loss spectroscopy, SIMS, ultraviolet photoemission, XPS, AES, and LEED. In addition, both electron-stimulated desorption and temperature-programmed desorption (TPD) studies are routinely performed in some systems. Typical information obtainable in TPD experiments includes the quantity and nature (intact or dissociated molecule) of an adsorbed gas. In addition, estimates of the sticking coefficient and the activation energy for desorption and/or reaction of the adsorbed molecule can be made. One of these systems has a combination of surface-science and high-pressure catalysis capabilities and is capable of measuring gas/solid reaction rates under realistic, high-pressure (approximately 1 atm) conditions using model, low-surface-area solid samples. Reaction rates as a function of temperature and varying reagent partial pressures also can be measured in this system.

Catalytic Reactors. The Reaction Engineering Laboratories are equipped with a variety of analytical capabilities and catalytic reactors including an Advanced Scientific Designs, Inc. RXM-100 catalyst testing and characterization instrument and a Zeton Altamira reactor test stand. The RXM-100, a multi-functional instrument used for catalyst studies, combines UHV and high-pressure capabilities in a single instrument without compromising specifications or ease of use. A number of measurements can be made using this instrument including chemical adsorption, physical adsorption, surface area, pore size, pore distribution, and temperature programmed characterization (desorption, reduction, and oxidation). An online mass spectrometer, gas chromatograph, FTIR, and thermal conductivity detector can be used to analyze effluent gases. The instrument has the capability of running up to 10 different gases simultaneously. In addition, high-pressure reactions (up to 1000 psi) can be run within a few minutes of each other on the same system, with little change in system configuration. This system offers extensive flexibility in catalyst testing and decreases inefficiency and contamination problems that arise from transferring materials between systems and waiting for data from other sources. The Zeton Altamira reactor test stand comprises three types of reactors generally used in bench-scale testing of catalysts: a fixed bed reactor, a Rotoberty reactor, and a continuous stirred tank reactor. This design allows users to evaluate catalyst performance and study chemical reactions in various reactor configurations.

X-Ray Diffraction. The suite of x-ray diffraction (XRD) equipment in EMSL consists of four instruments: a general-purpose XRD system for studying polycrystalline samples under ambient conditions, a special applications XRD system with low- and high-temperature sample stages covering the range of −193°C to +1000°C, and a four-circle XRD system. The general-purpose system is most often used to examine powder samples (x-ray powder

diffraction), but it also can be used to study certain types of thin films. In addition to its non-ambient capabilities, the special applications system is equipped to examine thin-film samples in more detail, including grazing-incidence XRD (GIXRD) and x-ray reflectivity (XRR) measurements. The four-circle system is typically configured for high-resolution x-ray diffraction studies of epitaxial thin films. Additional applications of the four-circle system include stress measurements, texture analysis, GIXRD, and XRR.

Chemically Selective Materials and Sensors. Development and evaluation of sensor materials and chemical microsensors are supported by a wet chemistry laboratory for organic, polymer, and nanomaterial synthesis; a laboratory for evaluation of chemical sensor and sensor materials using automated vapor generation and blending systems; and a clean room with selected microfabrication capabilities. A variety of techniques for applying sensing materials to sensor devices are available, and numerous electronic test instruments are available in the sensing laboratories and the EMSL Instrument Development Laboratory. These capabilities are complemented by a range of surface analysis and characterization instruments as well as conventional analytical instrumentation in EMSL. Users may wish to bring new sensing materials to EMSL for application to sensing devices and evaluation, while others may bring complete sensor systems with data collection capabilities to couple to EMSL automated vapor generation systems. Research areas include sensor arrays, sensor materials design and synthesis, sensing material/analyte interactions, and chemometric methods.

Microfabrication. Microfabrication equipment provides a significant research and development capability in the areas of microstructures, microsensors, and microanalytical systems. Unlike highly automated industrial production equipment, the microfabrication equipment in EMSL has multipurpose functionality. The equipment supports a variety of microprocessing activities that include thin-film deposition, various thermal treatments, microphotolithography, chemical etching, inspection and characterization, bonding and packaging, and testing and measurement.

Nanobiotechnology Laboratory. The Nanobiotechnology Laboratory is equipped with capabilities to synthesize single-enzyme nanoparticles, functionalize nanostructured matrices, and analyze the activity and stability of enzymes and single-enzyme nanoparticles. This new laboratory consists of various small instruments (such as a black box, a glove box, a Dean Stark system, and shakers), a spectrophotometer, and a spectrofluorometer. A variety of basic enzyme work can be performed in this laboratory, including enzyme modification, enzyme immobilization, and enzyme-activity and stability measurements.

Instrument Upgrades

Several instrument developments are being implemented or planned to enhance capabilities and support our major research areas or areas selected for EMSL development. In Fiscal Year 2006, the following capability developments and procurements occurred in the INSF.

- **Cryo-transmission electron microscope (TEM).** This new EMSL capability (Figure 5) adds major TEM capabilities for life sciences; three-dimensional reconstruction by TEM tomography will literally bring a new dimension into all structural analyses. This state-of-the-art technology is based on acquirement of tilt series of a specimen and its software reconstruction and rendering. The TEM cryo stage will allow visualization of cells and macromolecules in their native hydrated state by physical fixation within ultra-thin, vitrified ice layers. Gaining these capabilities leads to a whole new area of structural biology investigations at PNNL that has been so far limited to the conventional TEM imaging. This new instrument provides a vital tool for morphological and functional studies in the area of cell biology and proteomics.

Figure 5. Cryo-TEM.

- **Ultrahigh Vacuum Scanning Probe Microscopy.** A great need exists to establish experimental tools to obtain single-site chemical information that will lead to new knowledge important in several areas, such as heterogeneous catalysis and for important catalytic materials such as metal oxides. Ideally, one would like to obtain chemically specific information on the sub-nanometer scale. The INSF has developed an ultra-high vacuum system with non-contact atomic force microscope/scanning tunneling microscope capability along with several surface science techniques to obtain single-site chemical information. When the development effort first began, atomic force microscopy/scanning tunneling microscopy technologies readily allowed the variation of sample temperature, which EMSL instrumentation allowed. However, this instrumentation has a rather limited capability at low temperatures, because of issues with sample contamination. Only truly low-temperature ultra-high vacuum scanning probe microscopy where the entire microscope head is kept at low temperature would allow this problem to be overcome.

- **Elastic recoil detection analysis (ERDA) development.** Light element analysis is critical in several EMSL associated research areas, including oxide thin films for optical, magnetic, and catalytic materials and characterization of environmental and biological samples. The time-of-flight ERDA technique will provide simultaneous detection and absolute quantification of hydrogen, carbon, nitrogen, oxygen, and other light elements as a function of depth in complex matrices containing heavy elements, and, as a result, considerable attention is being devoted in developing this capability in ion beam facilities. Since this is a powerful method to investigate elemental concentrations in the

surface regions, this capability can be effectively applied to many different areas. This activity is almost complete, with a program associated with radiation detection materials development being worked and ready for users in Fiscal Year 2007.

- **Energy filtered imaging.** Electron energy loss spectroscopy for identification of light elements was developed, along with energy-filtered imaging with energy-specified electrons and electron diffraction capabilities. This capability development activity has been completed, and the capabilities are available for users.

- **Expert system for characterization of nanomaterials by x-ray photoelectron spectroscopy.** Development of this capability involved collaboration between the INSF and EMSL's Instrument Development Laboratory, and involves developing a software tool for faster and quantitative analysis of data from nanomaterials. This capability is not complete, and the facility is hoping to complete development by end of Fiscal Year 2007.

Future Directions

The overall objectives of the INSF are to support current highly productive users and user base and to expand outreach and capabilities related to developing areas associated with EMSL science themes and grand challenges. Accomplishments expected for Fiscal Year 2007 by this facility are as follows.

- **User support.** The facility's current user base is strong and productive. One objective is to maintain that base and the high level of user-produced output. The facility will also continue to make an impact in science themes and science theme-related calls, with significant contribution to the science theme call advertised in Fiscal Year 2006. The facility will work hard to obtain more than 20 science theme proposals during Fiscal Year 2007. The facility will also continue to work hard to update the user proposal database and convert most of the facility proposals to science theme proposals. The facility will continue to work to maintain/increase the total number of publications (110-120) with its distinguished and prominent user base. The long-term goal of the facility is to increase publications, especially in high-profile journals, and to increase the number of high-profile users.

- **Capability development.** As described below, significant new efforts are currently undertaken to enhance the support to all four EMSL science themes:

    - **Dual focused ion beam/scanning electron microscopy.** This new capability is crucial for the facility. Focused ion beams and two-beam focused ion beam/scanning electron microscopy systems are innovative instruments for nanoscience and engineering research that perform versatile tasks from prototyping novel architectures to materials analysis. The focused ion beam has revolutionized micromachining for the semiconductor device industry and is becoming a powerful tool in precise, cost-effective sample preparation of materials for transmission electron microscopy characterization. The facility will use the system's full capability

for nanomaterials synthesis and modification. This capability will include a cryo-stage so that biological samples can be successfully handled. In addition, the sample transfer system will help interface this capability with several other capabilities, including high resolution transmission electron microscopy, x-ray photon spectroscopy, and secondary ion mass spectrometry.

- **Time-of-flight secondary ion mass spectrometry.** Both biological systems and atmospheric chemistry research will be enhanced by a new generation of this capability, which will allow better depth resolution and extraction of information from environmentally unstable materials (biological and aerosol samples). Advances in the ion beam analysis capability will allow increased time resolution for atmospheric chemical analysis.

- **Catalytic reaction chamber for the quantum system.** This system will be connected to the existing Quantum x-ray photo spectroscopy system. It adds a new capability to Quantum and the planned capability will allow powder catalysis samples to be processed (heated in vacuum or in atmospheric pressure gas) before analysis by x-ray photon spectroscopy. This allows catalysts to be processed and analyzed without destroying information and minimizing changes to oxidation state. The same system will also have a higher-pressure reaction chamber where test catalytic reactions can be conducted and samples entered into the x-ray photon spectroscopy system, again without air exposure.

- **Hemispherical electron energy analyzer.** The ultrahigh vacuum scanning tunneling microscopy system will be upgraded with the high spatial and energy resolution hemispherical electron energy analyzer for examination of site specific chemical reactions. In general, the older analyzer analyzes a larger sample area. Experience has shown that the smaller sample size required compared to the sizes that could be analyzed by older analyzer. The new analyzer will be installed to do the smaller area analysis.

- **Ultra high vacuum processing chamber for Kratos AXIS system.** This capability will be crucial to process single crystals under ultra-high vacuum conditions for catalysis and photocatalysis studies. Sample quality and removal of contamination is a critical part of single crystal surface studies, including catalysis and photocatalysis. High-temperature sample heating, exposure to gases and sometimes plasmas are useful to accomplish this process. To heat samples to temperatures higher than allowed in the analysis chamber and allow exposure to higher gas pressures than desirable for the system, a modified existing chamber with sample manipulation capabilities would be connected to the Kratos AXIS system using the EMSL platen transfer approach.

- **Auger electron spectroscopy upgrade.** Two main instruments will be purchased and incorporated into a scanning Auger microscope. The first will involve an ion gun update to the Physical Electronics 680 Auger nanoprobe system, which will require a floating column design that generates high current densities at low beam energies and the ability to create low energy ion flood for use in sample neutralization. The second will involve a data acquisition system update to the Physical Electronics 680 Auger nanoprobe system.

- **Scanning multi-probe surface analysis system.** Very high demand exists for x-ray photoelectron spectroscopy analysis at EMSL. In addition, there are additional needs for state-of-the-art sputter depth profiling, in particular on biological samples and ultraviolet photoemission capability in conjunction with the x-ray photoelectron spectroscopy and depth profiling capability for organic samples. State-of-the-art sputter depth profiling of organic molecules, self assembled monolayers, and biological samples can be achieved by a new ion gun system based on ^{60}C. As such, a system will be developed in Fiscal Year 2007 that consists of ^{60}C ion gun sputter depth profiling capability and ultraviolet photoemission capability in addition to the small-spot x-ray photoelectron spectroscopy capability with high sensitivity.

Synthesis of Organically Templated Nanoporous Tin (II/IV) Phosphate for Radionuclide and Metal Sequestration

DM Wellman,[a] SV Mattigod,[a] KE Parker, [a] SM Heald,[a] C Wang, [b] and GE Fryxell[a]

(a) Pacific Northwest National Laboratory, Richland, Washington

(b) W.R. Wiley Environmental Molecular Sciences Laboratory, Richland, Washington

Effective removal of heavy metals and pollutants from the environment will lead to a clean living environment. Nanoporous materials offer an efficient way of selectively sequestering many types of metals and radionuclides in a very small volume. The high-surface area of a nanoporous structure enhances mass transfer in sequestration applications and enables ions to be highly concentrated in a very small volume of material. Operations related to nuclear energy and weapons production have produced significant quantities of radioactive waste during the last half century that will be processed and buried in a deep geological repository at Yucca Mountain in Nevada. The current proposal is to include "getter materials" with this waste to sequester any radionuclides that might leach from the waste forms. Of particular interest are the long-lived actinide species (e.g., plutonium, americium, neptunium) and the anions (e.g., pertechnetate, iodide). Getter materials must be able to survive long-term exposure to elevated temperatures (>150°C) and moderately high radiation fluxes. The frailty of organic components towards radiolytic degradation precludes their use for either structure or function in the final getter material.

During the last decade, metal phosphates have been extensively studied for their potential use in catalysis, ion exchange, and phase separation. Since the first open-framework tin phosphates were prepared nearly 15 years ago, there has been interest in the structural flexibility of tin phosphates crystallizing in one-dimensional, three-dimensional, or layered structures. Open-framework tin phosphates have been prepared by direct precipitation and by incorporating organic amines into the crystal lattice. Surfactant-templated, open-framework tin phosphates have been reported using structure directing amine compounds including ethylenediamine, 1,6-diaminohexane, 1,2-diaminopropane, 1,8-diaminooctane, and 1,4-diaminobutane. Only recently, however, has a nanoporous tin (IV) phosphate been reported, and, to date, this is the only known report of a nanoporous tin phosphate. The cationic quaternary ammonium salt $CH_3(CH_2)_{15}N(CH_3)_3Br$ was used as the surfactant. The use of cetyltrimethylammonium bromide as surfactant resulted in surface areas of 230 m^2/g and pore sizes of 35-38 Å. Although the pore size was reduced from 39 to 35 Å, the structure was stable following calcination.

The goal of this study was to produce a similarly stable, mesoporous solid using tin (II) as the starting material to produce a material capable of sequestering redox-sensitive species, such as pertechnetate, neptunium, chromium, and iodide. The large pores afforded with quaternary ammonium surfactants and the high-surface area of nanoporous structures are valuable features for enhanced mass transfer in sequestration applications. This work summarizes efforts to make a nanoporous tin(II) phosphate phase. The synthesis method consists of preparing 200 mL of 6.87 mmol cetyltrimethylammonium chloride $CH_3(CH_2)^{15}N(CH_3)^3Cl$, in deionized water. The solution is acidified with 0.626 mL of concentrated phosphoric acid. A concentrated solution of 15.22-g stannous chloride was dissolved in 100-mL hydrochloric acid. 2.5 mL of $SnCl^2$/HCl solution was added with stirring at room temperature to the acidified surfactant. The solution stirred for 30 minutes at room temperature and was placed in an oven at 65°C for 48 to 72 hours. The synthetic material was collected via vacuum filtration using a 0.45-μm filter, washed with deionized water, and dried under ambient conditions. Chemical analysis of the synthetic material indicates the structure is composed of Sn:P:O with a ratio of 1:1:5.

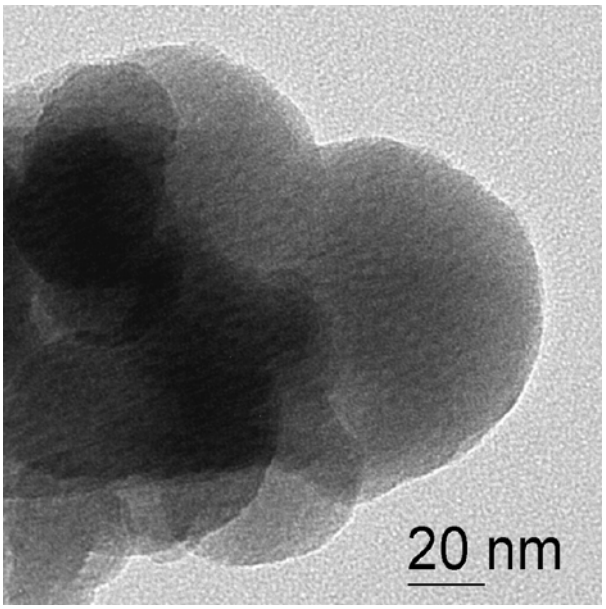

Figure 1. Calcination of the as-synthesized material at 500°C produced a material with a surface area of 262 m^2/g. The x-ray diffraction pattern of the surfactant-$SnPO_4$ and calcined $SnPO_4$ are shown above. The d spacing of the 100 plane in surfactant-$SnPO_4$ is 5.01 nm, whereas after calcination it was reduced to 4.62 nm. Subjecting the nanoporous $SnPO_4$ (NP-SnPO) to high temperatures during calcination has little impact on pore size.

Selected-area electron diffraction analysis of a typical tin phosphate (NP-SNPO) illustrates a completely amorphous structure. Analyses with high-resolution transmission-electron microscopy revealed a spherical particle morphology approximately 150 nm across, with uniform pore distribution narrowly distributed around 2 nm. It was also observed that directly precipitated NP-SNPO materials, in addition to being thermally stable (500°C), are chemically stable over the entire pH range (pH = 0 to 14); therefore, tin will not leach into water during remediation operations (Figure 1).

Preliminary batch contact studies have been conducted to assess the effectiveness of NP-SnPO in sequestering redox-sensitive metals and radionuclides, technetium(VII), neptunium(V), thorium(IV), and a toxic metal, chromium(VI), from aqueous matrices. Equilibrium was achieved in less than an hour at a solution-to-solids ratio of 100, therefore a

batch contact time of 2 hours was used to ensure that these values represent true equilibrium conditions. Under these conditions, the nanoporous, calcined tin (II) phosphate removed >95% of all contaminants investigated from solution. Distribution coefficients, Kd, are defined as a mass-weighted partition coefficient. Kd values were typically >10,000 in groundwater for the nanoporous tin (II) phosphate; whereas, Kd values for non-porous tin (II) phosphate was ~100. At a solution-to-solids ratio of 100, a Kd value of 10,000 indicates that at equilibrium there was 100 times as much contaminant in the nanoporous metal-phosphate phase as there was remaining in the supernantant solution.

Data obtained via x-ray absorption near edge spectra/extended x-ray absorption fine structure analysis clearly illustrate the sequestration of Tc(VII), Np(V), and Cr(VI) with NP-SNPO occurs through redox-coupled reactions with the target metals being reduced to their least soluble valence states, namely, Tc(IV), Np(IV), and Cr (III), with oxidation of tin in NP-SnPO. Although lacking spectroscopic data, we surmise that Th(IV) adsorption on NP-SnPO is due to Lewis acid-base interaction with PO_4 groups.

These nanoporous tin (II) phosphates exhibited significant promise as sorbent materials for anionic and redox-sensitive metals and actinides. The detailed kinetic studies of these materials are planned for publication.

A Soft X-ray Absorption Spectroscopy Study of Ceria Grown on Al_2O_3(0001)

P Nachimuthu,[a] LV Saraf,[b] C Wang,[b] V Shutthanandan,[b] DE McCready[b] S Thevuthasan,[b] DK Shuh,[c] DW Lindle,[a] and RCC Perera[c]

(a) University of Nevada, Las Vegas, Nevada

(b) W.R. Wiley Environmental Molecular Sciences Laboratory, Richland, Washington

(c) Lawrence Berkeley National Laboratory, Berkeley, California

Both O 1s and Ce 3d x-ray absorption spectra show that ceria films with particle sizes of 3 nm and 7 nm are largely oxygen deficient. As a result, a significant amount of trivalent cerium ions are present in the ceria films, whereas the ceria film with a particle size of 38 nm is fairly stoichiometric CeO_2. Furthermore, the ^{18}O intake measurements of ceria films show that the redox potential of Ce^{3+}/Ce^{4+} ions is flexible enough such that the nanocrystalline ceria is stable at room temperature and can be manipulated for specific applications, such as catalysis.

Ceria-based oxides are being used as catalysts in many technological applications because of their unique redox properties. The overall performance of these oxides depends on particle size, structural characteristics, and chemical nonstoichiometry. Most applications for the ceria-based oxides are surface sensitive, and recent advances in nanotechnology enable fabrication of these oxides as nanostructures. These nanostructures can be used to reach a high surface-to-volume ratio, in addition to improved redox properties, related to oxygen vacancy generation. Therefore, a detailed scientific understanding of the growth and characterization of ceria nanostructures becomes necessary to determine viability of these

materials for various applications. In this study, we investigated the oxidation state and local structure of ceria grown on $Al_2O_3(0001)$ single crystal surfaces with different particle sizes prior to and following oxygen intake using soft x-ray absorption spectroscopy.

The O 1s and Ce 3d x-ray absorption spectra of ceria films measured at Beamline 6.3.1 of the Advanced Light Source at Lawrence Berkeley National Laboratory are shown in Figure 1. The prominent features in the O 1s spectra are a sharp pre-edge transition at 530 eV and an intense transition at 532.5 eV, which is superimposed on the edge jump, and a broad band centered at 536.9eV. The sharp pre-edge transition at 530 eV arises from the excitation of O 1s core electrons to 2p hole-states in the narrow 4f dominated bands resulting from strong Ce 4f and O 2p hybridization in the ground states of CeO_2. Similarly, the intense transition at 532.5 eV and the broad band at 536.9 eV are assigned to the transitions from O 1s to Ce $5d(e_g)$ and $5d(t_{2g})$ states, respectively, while the edge jump corresponds to transitions to empty continuum states. It can be noted from Figure 1a that the intensities of the transitions at 530 eV, 532.5 eV, and 536.9 eV in the O 1s spectra collected at both $\theta=0^o$ and $\theta=82.5^o$ increase with increasing the particle size of ceria films from 3 nm to 38 nm. This intensity increase for the transition at 530 eV amounts to ~19% and ~17% for the spectra recorded at $\theta=0^o$ and 82.5^o, respectively. For transitions at 532.5 eV and 536.9 eV, the intensity increase is 7% each for the spectra recorded at both $\theta=0^o$ and 82.5^o. In general, the electronic transitions in the x-ray absorption spectra occur from a selected atomic core

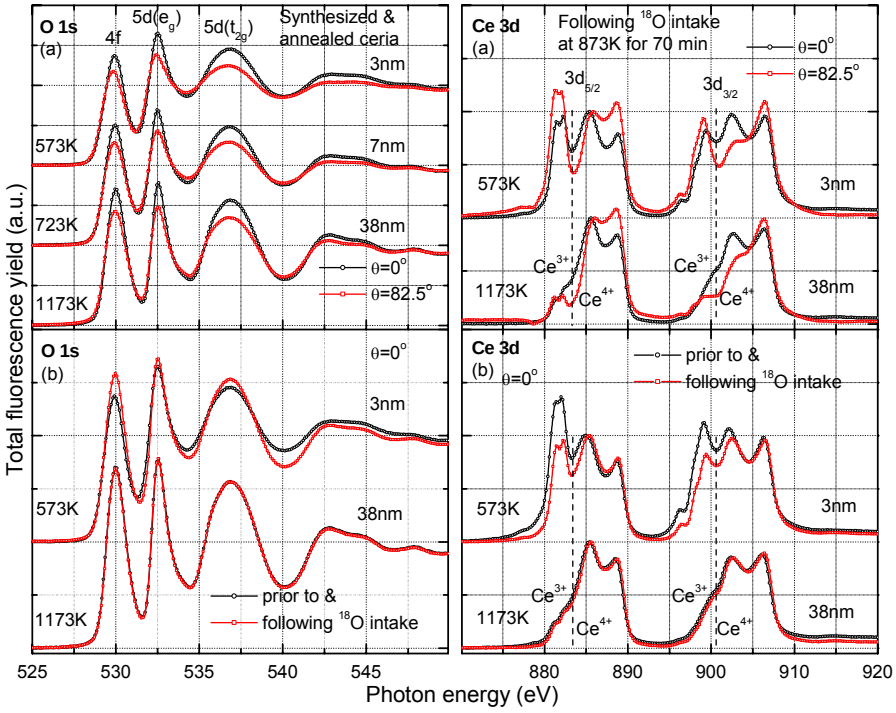

Figure 1. (a) Comparison of the normal ($\theta=0^o$) and grazing incidence ($\theta=82.5^o$) x-ray absorption spectra at O 1s and Ce 3d edges from ceria films on $Al_2O_3(0001)$ with particle sizes of 3 nm, 7 nm, and 38 nm. (b) The normal incidence ($\theta=0^o$) x-ray absorption spectra at O 1s and Ce 3d edges from ceria films on $Al_2O_3(0001)$ with particle sizes of 3 nm and 38 nm prior to and following ^{18}O intake by annealing the films in 4.0 x 10^{-6} Torr of $^{18}O_2$ at 873 K for 70 min.

level to unoccupied states and intensities of these transitions are directly related to the unoccupied density of states, which results from the chemical and electronic structures of a given chemical composition.

The x-ray diffraction and high-resolution transmission electron microscopy results show that the ceria annealed at 573 K and 723 K retain nanocrystalline phases, while the ceria annealed at 1173 K reveal characteristics of polycrystalline CeO_2. The intensity increase in the O 1s spectra suggests that the nanocrystalline ceria films with lower particle sizes are oxygen deficient, which leads to the formation of Ce^{3+} in the ceria films. With increasing annealing temperature, the oxygen-deficient nanocrystalline ceria films absorb oxygen from air, which facilitates the oxidation of Ce^{3+} to Ce^{4+} with increased bond formation leading to increased particle size and long-range ordering. Comparison of these O 1s spectra with the spectra from reference materials suggests that the pre-edge transition at 530 eV is originated from CeO_2, whereas the transitions at 532.5 eV and 536.9 eV can originate from oxide ions coordinated to both Ce^{3+} and Ce^{4+}. A moderate increase in intensity (~7%) for the transitions at 532.5 eV and 536.9 eV with increasing particle size of ceria films only suggests an increase of long-range ordering of the ceria film with annealing temperature, assuming that the fluorescence cross sections of oxide ions coordinated to Ce^{3+} and Ce^{4+} are the same. A drastic increase in intensity (19%) for the pre-edge transition at 530 eV shows the presence of Ce^{3+} in ceria film with lower particle size and it is being oxidized to Ce^{4+} in addition to increase of long-range ordering with increasing particle size of ceria films.

Furthermore, the intensities for all transitions in the O 1s spectra collected at $\theta=82.5^{o}$ are significantly reduced (14%) compared to the spectra at $\theta=0^{o,}$ regardless of ceria particle size (Figure 1b). These ceria films do not show polarization dependence because of the lack of specific orientation; however, the probing depth at $\theta=0^{o}$ is up to 300 nm, and it is restricted to only the near-surface region at $\theta=82.5^{o}$. Therefore, the difference between the spectra collected at $\theta=0^{o}$ and $\theta=82.5^{o}$ results from the variation of ceria surface from its bulk. A reduction in intensity for grazing incidence spectra suggests more oxygen deficiency and a lack of long-range ordering in the near-surface region compared to the bulk ceria film.

The O 1s x-ray absorption spectra collected at $\theta=0^{o}$ from ceria films with a particle size of 3 nm show an increase in intensity for all transitions following ^{18}O intake. However, the increase in intensity for the transition at 530 eV is significant as this transition is characteristic of CeO_2 and is sensitive to oxygen deficiency. These results suggest that the ceria film with a particle size of 3 nm is oxygen deficient and takes more oxygen when subjected to annealing at high temperature in an oxygen atmosphere. In contrast, the spectra for the ceria film with a particle size of 38 nm prior to and following annealing the films in $4.0x10^{-6}$ Torr of $^{18}O_2$ at 873K for 70 minutes show no changes, suggesting that this ceria film is stoichiometric CeO_2.

In the Ce 3d x-ray absorption spectra collected at $\theta=0$ and $\theta=82.5$ from ceria films grown on $Al_2O_3(0001)$ with particle sizes of 3 nm, 7 nm, and 38nm, the transitions occur from the initial $3d^{10}4f^{n}$ state to the final states of the form $3d^{9}4f^{n+1}$. Spin-orbit interaction splits the Ce 3d into $3d_{5/2}$ and $3d_{3/2}$ states separated by ~17.6 eV. The spectra reflect the oxidation states of Ce in ceria films with different particle size. Based on the spectra from reference materials, the transitions originating from Ce^{3+} and Ce^{4+} are separated with dashed lines in

both the $3d_{5/2}$ and $3d_{3/2}$ edges of Ce. The energy separation between Ce^{3+} and Ce^{4+} in ceria films corresponds to ~3.0eV. The intensities of the transitions originating from Ce^{3+} relative to the intensities of the transitions originating from Ce^{4+} decrease for the spectra recorded at both $\theta=0^{o}$ and $\theta=82.5^{o}$ from ceria films with increasing particle size, suggesting that the relative concentrations of Ce^{3+} ions decrease. Furthermore, the relative intensities of the transitions originating from Ce^{3+} is larger for the spectra recorded at $\theta=82.5^{o}$ compared to the spectra recorded at $\theta=0^{o}$ regardless of the particle size of the ceria film, suggesting that the relative concentrations of Ce^{3+} on the surface is larger than in the bulk of the ceria film with a specific particle size. Ceria on the surface is also more susceptible to reduction by x-ray, especially when the particle sizes are smaller, because of their larger surface area with no or reduced long-range ordering. These results are in good agreement with those obtained from O 1s spectra.

The intensities of the transitions originating from Ce^{3+} relative to the intensities of the transitions originating from Ce^{4+} are significantly reduced for the spectra recorded from ceria film with particle sizes of 3 nm following ^{18}O intake, compared to the spectra recorded prior to ^{18}O intake. These results suggest that the Ce^{3+} present in the ceria film with particle sizes of 3 nm prior to ^{18}O intake is oxidized to Ce^{4+} following ^{18}O intake. However, the spectra recorded from ceria film with particle sizes of 38 nm prior to and following ^{18}O intake show no changes, suggesting that this ceria film does not have significant concentrations of Ce^{3+}. These results are also consistent with those obtained from O 1s spectra.

Geophysical Imaging of Stimulated Microbial Biomineralization

KH Williams,[a,b] D Ntarlagiannis, [c] LD Slater,[c] A Dohnalkova,[d] SS Hubbard,[b] and JF Banfield [a][b]

(a) University of California, Berkeley, California
(b) Lawrence Berkeley National Laboratory, Berkeley, California
(c) Rutgers University, Newark, New Jersey
(d) W.R. Wiley Environmental Molecular Sciences Laboratory, Richland, Washington

Understanding how microorganisms influence the physical and chemical properties of the subsurface is hindered by our inability to observe microbial dynamics in real time and with high spatial resolution. Here, we investigate the use of noninvasive geophysical methods to monitor biomineralization at the laboratory scale during stimulated sulfate reduction under dynamic flow conditions. Geophysical data reflected the distribution of mineral precipitates and biomass over space and time, with temporal variations in the signals corresponding to changes in the aggregation state of the nanocrystalline sulfides. These results were correlated with data obtained by transmission and scanning electron microcopy. The results suggest the potential for using geophysical techniques to image certain subsurface biogeochemical processes, such as those accompanying the bioremediation of metal-contaminated aquifers.

The problem of groundwater contamination by acid-mine drainage, industrial sources, and government nuclear weapons programs has spawned interest in the ability of microorganisms to facilitate remediation through sequestration of metals in insoluble precipitates. High-resolution geophysical techniques have proven extremely useful at the field scale for estimating hydrogeological properties, providing information about subsurface environments. In this study, the sensitivity of two geophysical techniques, complex resistivity and acoustic wave propagation, is tested to the products of microbial biomineralization. The primary objective was to follow the reaction dynamics of a column-scale biostimulation experiment using conventional biogeochemical and mineralogical measurements, as well as noninvasive geophysical techniques. We tested the hypothesis that metal sequestration via microbe-induced sulfide precipitation creates physical property changes that directly alter the response of geophysical signals. We compared the temporal response of such signals against concomitant changes in fluid chemistry and microbial biomass to investigate if the geophysical responses are sensitive to the products of biomineralization. Finally, we validated our interpretation of the geophysical responses using electron microscopy techniques.

Sulfate-reducing bacterium *Desulfovibrio vulgaris* was used for monitoring of microbe-induced ZnS and FeS precipitation within saturated sand-packed columns. Acoustic wave measurements and saturated hydraulic conductivity measurement were done during the duration of the experiment. Columns were terminated after 78 days and analyzed for concentration of sediment-affixed metal sulfides and microbial biomass. Solution samples from the influent, effluent, and multiport samplers were analyzed for major dissolved

components at 3- to 5-day intervals. Total dissolved zinc and iron was determined by inductively coupled plasma atomic emission spectroscopy. Lactate, acetate, and sulfate concentrations were determined by gradient elution ion chromatography. Solution pH was measured using a sulfide-tolerant electrode. Transmission and scanning electron microscopy were used for characterizing microbe-mineral associations and the crystal size and aggregation state, and they documented significant spatial variability in the abundance and distribution of cells and their associated mineral products. Transmission electron microscopy-based analysis of the precipitates revealed them to be a mixture of sphalerite (ZnS) and mackinawite (FeS), with an average crystal size of 3 nm (Figure 1). Scanning electron microscopy revealed grain coatings consisting of dense accumulations of sulfide-encrusted microbes.

We have shown that the stimulation of sulfate-reducing microorganisms and the associated formation of insoluble metal sulfides create physical property changes that are directly detectable using geophysical techniques. We have resolved spatiotemporal changes in complex resistivity and acoustic wave propagation resulting from variations in the electric charge-carrying capacity and elastic moduli of precipitates and pore fluids. The changes persisted over time and were confined exclusively to those regions where metals were sequestered in insoluble precipitates. Temporal changes in the geophysical signals appear to offer insight into the aggregation state of the sulfides and may be indicative of pore-scale crystal growth and aging, with such a result having implications for the fate and transport of microbe-induced precipitates. Our laboratory results are relevant to the larger spatial scales of the natural environment where methods currently used for field-scale geophysical monitoring may be used in an analogous fashion. These results show the potential of using complex resistivity and acoustic wave techniques for remotely monitoring regions of contaminant sequestration via biomineralization and for evaluating the overall long-term stability of such precipitates.

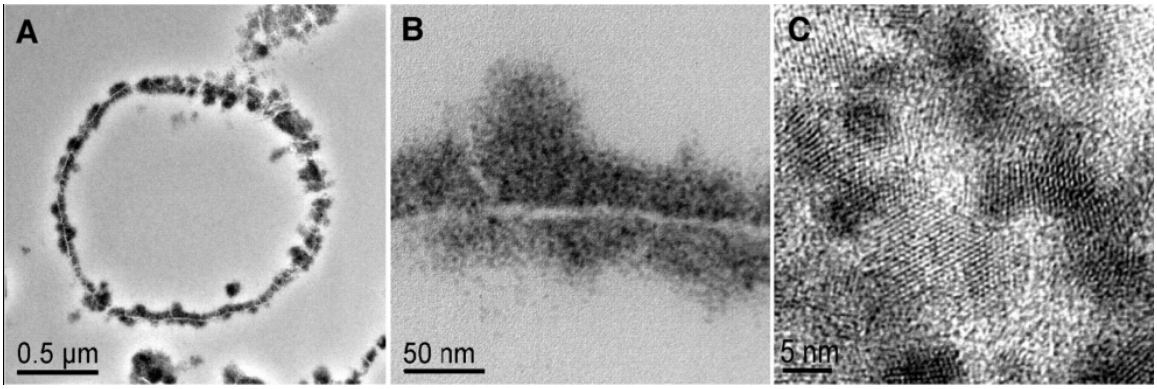

Figure 1. (A and B) Cross-sectional transmission electron microscopy images of a single *D. vulgaris* cell with membrane-bound ZnS and FeS precipitates. (C) High-resolution transmission electron microscopy revealed the nanocrystalline character of the precipitates with a typical particle size of 3 to 5 nm.

Kinetics of Electron-Beam-Enhanced Recrystallization of Amorphous Strontium Titanate

Y Zhang,[a] J Lian,[b] CM Wang,[a] RC Ewing,[b] and WJ Weber[c]

(a) W.R. Wiley Environmental Molecular Sciences Laboratory, Richland, Washington

(b) University of Michigan, Ann Arbor, Michigan

(c) Pacific Northwest National Laboratory, Richland, Washington

Single crystal strontium titanate ($SrTiO_3$) is of technological interest in microelectronics industries because of its high dielectric constant, good insulating properties, outstanding wear resistance, high oxidation resistance, and chemical and thermal stability. Strontium titanate thin films are used as insulating layers in dynamic random access memories, ferroelectric thin-film structures, and high-T_c superconductor devices, as well as potential gate oxide candidates. Strontium titanate and other titanate ceramics have also been proposed as phases for immobilization of nuclear waste. In many of these applications, knowledge of dynamic recovery and nanostructure evolution is critical.

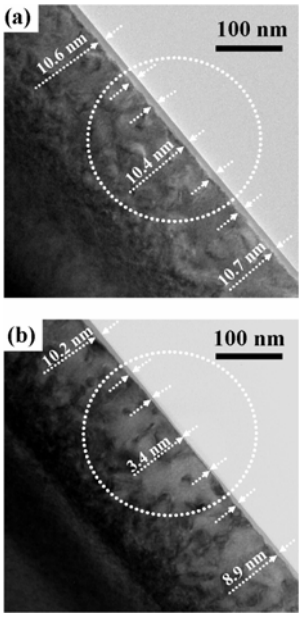

Figure 1. TEM images of sample A: (a) the amorphous layer. (b) recrystallization of amorphous layer following the *e*–beam irradiation.

Irradiation of $SrTiO_3$ with 1.0 MeV Au at 400 K leads to formation of an amorphous surface layer. In this research, the damage and microstructural features in the samples were investigated by Rutherford back-scattering spectroscopy and high-resolution transmission electron microscopy (TEM) images, and the results show amorphous regions of ~10.6 nm and ~330 nm for sample A, as shown in Figure 1(a), and sample B, respectively. Following exposure of the amorphous layers to TEM electron-beam (*e*-beam), the amorphous thickness decreases with exposure time, and *in situ* epitaxial recrystalli-zation at the amorphous/ crystalline (a/c) interface is observed, as shown in Figures 1(b) and 2. In the central area of the cross-sectional TEM image of sample A in Figure 1(b) where the *e*-beam is the most intense, more amorphous material recrystallizes, and the a/c interface moves toward the surface. At both edges of the cross-sectional image where the *e*-beam density is lower, recrystallization is not as significant. This indicates a strong dependence of the recrystallization process on *e*-beam flux. The *e*-beam-induced recrystallization of the amorphous layer in sample B is shown in Figure 2, where rapid *in situ* recrystallization at the a/c interface is evident.

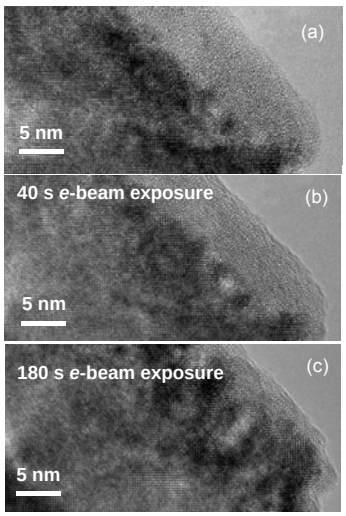

Figure 2. The a/c interface motion under *e*–beam exposure with flux of 5.0 $\times 10^{20}$ $cm^{-2}s^{-1}$.

The *in situ* recrystallization of the amorphous layer at room temperature under different beam flux is summarized in Figure 3. The solid phase regrowth appears as a series of linear stages with decreasing slopes as exposure time increases, resembling a sublinear-like regrowth behavior. In general, the recrystallization rate resulting from *e*-beam irradiation can be separated into three stages. During the initial stage (i.e., up to ~100 s), there exist many ion-induced defects near the a/c interface. Rapid motion at the a/c interface is observed, and the recrystallization processes proceed at a high rate. This fast recrystallization may be attributed to *e*-beam-enhanced defect annihilation at the a/c interface. Under the high *e*-beam flux (5.0 and 7.8 $\times 10^{20}$ $cm^{-2}s^{-1}$), the recrystallization processes during the initial stage occur very quickly, and no data were obtained during the very short durations. After the initial stage, during which most ion-induced defects were annealed out, the recrystallization rates become constant, and the recrystallization processes occur in a second stage. A well-defined linear relationship is observed for different fluxes at this stage. As the exposure time increases, little motion is observed at the a/c interface, and the recrystallization processes reach a saturation stage. The TEM observations indicate that the saturation stage occurs when the thickness of the amorphous layer is ~3 nm, which suggests that the surface may play an important role in stabilizing this final stage. It is evident in Figure 3 that the regrowth rate during the second stage increases with increasing beam flux from 1.2 to 5.0 $\times 10^{20}$ $cm^{-2}s^{-1}$, and shows no further increase with the increasing flux.

The regrowth rates in the second linear stage under *e*-beam irradiation were investigated as a function of flux and temperature. The *e*-beam enhanced recrystallization rates are orders of magnitude higher than those expected from thermal epitaxial recrystallization. Based on the temperature dependence of the recrystallization rates, an activation energy of 0.1±0.05 eV was determined for the *e*-beam-enhanced recrystallization processes. A sublinear-like regrowth dependence on exposure time may be used as a fingerprint for the *e*-beam enhanced recrystallization, as opposed to the superlinear-like behavior normally observed in thermal recrystallization.

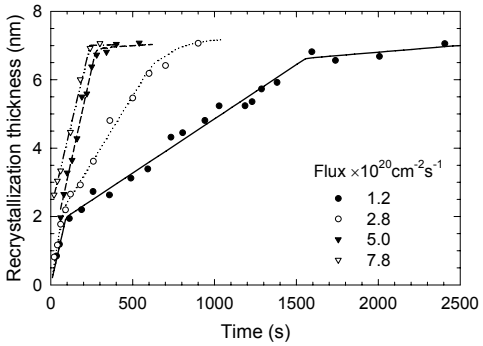

Figure 3. Solid phase regrowth of a/c transition as a function of exposure time to the *e*–beam under different fluxes.

During *e*-beam irradiation, the incident electrons primarily transfer energy by ionization processes that produce localized electronic excitations. The localized electronic excitations affect local atomic bonds and may effectively lower the energy barriers to recrystallization processes, which may involve local atomic hopping or rotation of atomic polyhedra.

Room-Temperature, Solvent-Free Synthesis of Monodisperse Magnetite Nanocrystals

XR Ye,[a] C Daraio,[a] CM Wang,[b] JB Talbot,[a] and S Jin[a]

(a) University of California-San Diego, La Jolla, California

(b) W.R. Wiley Environmental Molecular Science Laboratory, Richland, Washington

Magnetic nanoparticles are useful for a variety of scientific and technological applications such as magnetic storage media, ferrofluids, magnetic refrigeration, magnetic resonance imaging, hyperthermic cancer treatment, cell sorting, and targeted drug delivery. Iron oxides constitute one of the most fascinating classes of magnetic materials and have been extensively investigated. Based on chemical reactions in liquid or aerosol/vapor phases, different approaches such as coprecipitation, sol-gel, aging, ultrasound irradiation, and laser pyrolysis, have been established for preparing super-paramagnetic iron oxide nanoparticles typically smaller than 20 nm that are adaptable to variable applications. However, the relatively poor size uniformity and crystallinity of the nanoparticles obtained strongly affect their magnetic properties.

In this highlight, we report, for the first time, a novel, facile, and solvent-free synthetic method that allows the use of inorganic ferrous and ferric solids, along with surfactants, to produce monodisperse magnetite nanocrystals. The reaction is advantageous in that it is induced at room temperature rather than at the refluxing temperatures of ~265 to 350°C used in the typical organic-solution phase decomposition method in which organic iron is dissolved in organic solvents. Highly crystalline and monodispersed Fe_3O_4 nanocrystalline particles are obtained by the new process despite the fact that the reaction occurs at room temperature. Such a solvent-free reaction provides a substantial environmental advantage in that it eliminates the need for disposing of or recycling toxic chemicals. A solvent-free approach based on solid-state reactions was previously used for simple synthesis of unassembled nanoparticles; however, no surfactant was used for particle size control.

Solvent-free synthesis of magnetite nanocrystals can be considered as a hybrid of solid-state reaction, co-precipitation, and organic solution-phase decomposition processes that take advantage of only the beneficial parts of these processes. In this approach, the following modifications were made: 1) inorganic ferrous, ferric, and base solids were used directly for the synthesis rather than aqueous or organic solutions; 2) an oleic acid-oleylamine adduct solid was used as the surfactant stabilizer rather than oleic acid and oleylamine liquids; 3) after the reaction, the Fe_3O_4 nanoparticles were extracted directly into hexane, and the unreacted materials and the byproducts were separated conveniently since they are insoluble in hexane; and 4) mono-dispersed, uniform Fe_3O_4 nanoparticles that can be assembled into ordered arrays were obtained. In addition, this method requires no complex apparatus and techniques, and enables one to synthesize Fe_3O_4 nanocrystals with almost uniform size in high yields and at a large scale. The reaction, if carried out in the presence of a surfactant such as oleic acid-oleylamine adduct, generated monodisperse Fe_3O_4 nanocrystals extractable directly from the reaction mixture. The extracted nanoparticles were capable of forming a self-assembled, two-dimensional, and uniform periodic array. The new process uses inexpensive and nontoxic starting materials, and does not require a use of high-boiling-point

toxic solvents, so it is amenable to an environmentally desirable, large-scale synthesis of nanocrystals.

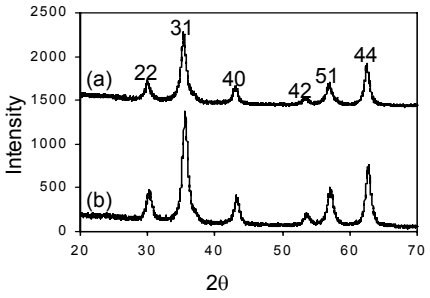

Figure 1. X-ray diffraction patterns of the nanoparticles.

X-ray diffraction patterns of the nanoparticles synthesized by the solvent-free reactions with and without the addition of oleic acid-oleylamine adduct are compared in Figure 1. Both patterns indicate the crystalline nature of the products, and the positions and relative intensities of all diffraction peaks coincide with those of the Joint Committee for Powder Diffraction Studies card (19-0629) for Fe_3O_4. No characteristic peaks of reactants and byproducts (mostly NaCl) were observed. The general transmission electron micrograph of the nanoparticles synthesized by the solvent-free reaction in the presence of surfactant is shown in Figure 2 (left image). The nanoparticles appear almost spherical and monodispersed with an average diameter of 5 nm, and self assemble into a two-dimensional array. A high-resolution transmission electron micrograph of the patterned nanoparticles is shown in Figure 2 (right image). The lattice spacing seen in the lattice fringe of the particles revealed the satisfactory crystallinity and structural uniformity of the sample.

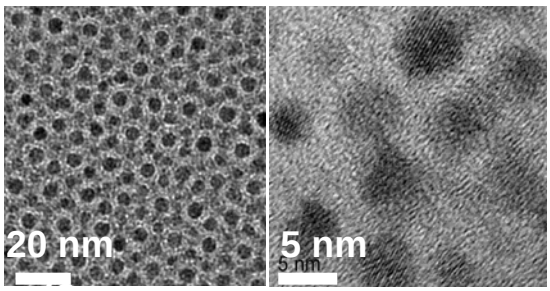

Figure 2. Transmission electron micrographs

We have successfully demonstrated and documented the synthesis of monodisperse Fe_3O_4 nanocrystals using a novel and easy one-step, solvent-free reaction (Ye et al. 2006). The reaction of the solvent-free synthesis in the presence of a surfactant is believed to precede a similar intermediate process via the formation of Fe(III) and Fe(II)-surfactant complexes. The reaction can be conveniently carried out at ambient temperature, thereby avoiding the use of toxic solvents with high boiling points. This technique, which uses inexpensive and nontoxic inorganic ferrous and ferric salts that are reacted at ambient temperature, is amenable to convenient, large-scale synthesis. With proper choices of inorganic metal salts and surfactants, this method may be extended to environmentally desirable preparation of a wide variety of monodisperse nanocrystals.

This research is described in more detail in Ye et al. 2006.

Citation

Ye X, C Daraio, C Wang, JB Talbot, and S Jin. 2006. "Room Temperature Solvent-Free Synthesis of Monodisperse Magnetite Nanocrystals." *Journal of Nanoscience and Nanotechnology* 6(3):852-856.

Identification of Isotopically Primitive Interplanetary Dust Particles

C Floss,[a] FJ Stadermann,[a] JP Bradley,[b] ZR Dai,[b] S Bajt,[b] G Graham,[b] and SA Lea[c]

(a) Washington University, St. Louis, Missouri
(b) Institute for Geophysics and Planetary Physics, Livermore, California
(c) W.R. Wiley Environmental Molecular Sciences Laboratory, Richland, Washington

Interplanetary dust particles (IDPs), which originate largely from comets and asteroids, are complex assemblages of various primitive solar system materials. Chondritic porous IDPs are dominated by anhydrous minerals, in contrast to chondritic smooth IDPs that are composed predominantly of hydrated layer lattice silicates. While specific parent bodies are not known, hydrated IDPs have been linked to asteroidal origins, whereas anhydrous IDPs may be more likely to have cometary origins.

Isotopic measurements of IDPs show the presence of abundant extra-solar phases. Significant depletions and enrichments in hydrogen isotopic compositions have been found in IDPs and almost certainly have an interstellar origin. The origin of nitrogen isotopic anomalies is more complicated than that of hydrogen, because nitrogen isotopic fractionation has not been observed in the interstellar medium and anomalous nitrogen can also have a nucleo-synthetic origin. However, recent theoretical work shows that chemical reactions in dense molecular clouds can produce elevated $^{15}N/^{14}N$ ratios.

High spatial resolution surface analytical instrumentation such as NanoSIMS and scanning auger microscopy have the ability to make isotopic measurements and identify mineralogical phases at the sub-micron scale, providing renewed opportunities to investigate the compositions of IDPs. Our goal has been to gain a better understanding of the abundance, nature, and distribution of isotopically anomalous phases in IDPs and, thereby, constrain both the nature of these phases and the parent bodies from which IDPs originate.

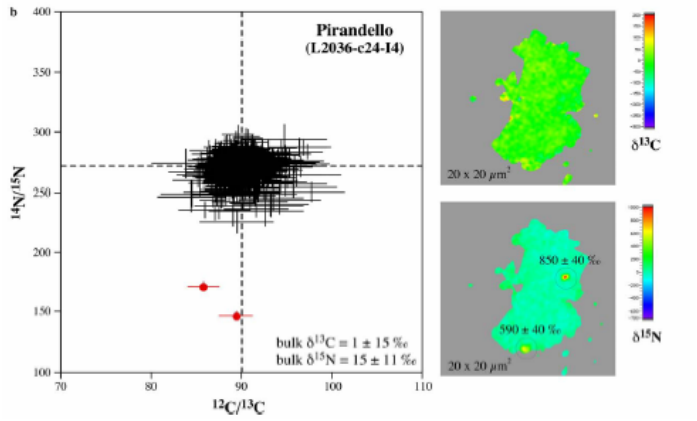

Figure 1. Carbon and nitrogen isotopic compositions of Pirandello from NanoSIMS analysis. Shown are isotope plots of the $^{12}C/^{13}C$ and $^{14}N/^{15}N$ ratios of 500 nm-sized subregions of the IDPs and false color images of the $\delta^{13}C$ and $\delta^{15}N$ compositions of the particles. Pirandello has isotopically normal bulk compositions in carbon and nitrogen, but contains two hot spots enriched in ^{15}N. Dashed lines show terrestrial carbon and nitrogen ratios.

Carbon and nitrogen isotopic compositions were measured in 39 IDPs from NASA collector flags L2009, L2011, and L2036. Hydrogen isotopic compositions were measured in a subset of these 39 IDPs. Typical data collected from these 39 IDPs, using NanoSIMs imaging and scanning Auger microscopy, are shown in Figure 1.

Auger elemental maps of pre-solar grain D1 from the IDP Deledda show that it is an iron-rich silicate (Figure 2). Iron-magnesium silicates, such as olivine and pyroxene, are expected to have magnesium-rich compositions under conditions of equilibrium condensation in the stellar winds of oxygen-rich RGB and AGB stars. Deledda appears to be an anhydrous IDP, which is unlikely to have experienced significant secondary processing. Thus, the pre-solar grain D1 may represent a primary iron-rich silicate condensate that formed under nonequilibrium conditions.

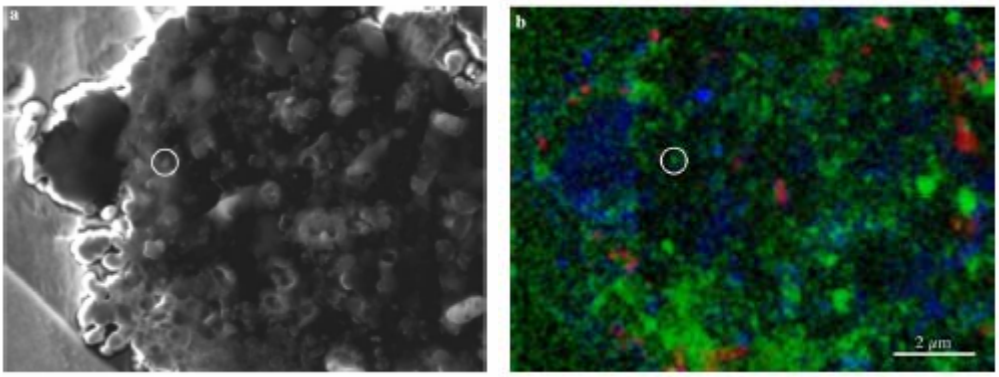

Figure 2. Auger elemental maps of presolar grain D1 from the IDP Deledda.

Isotopic imaging of a suite of IDPs shows that nitrogen isotopic compositions can be used to characterize IDPs and identify those that share a variety of primitive isotopic compositions, including the presence of abundant pre-solar silicate grains (Floss et al. 2006). Hydrogen and nitrogen isotopic compositions in these IDPs show similar distributions; fractionations are present both as small D-rich or ^{15}N-rich hot spots and as larger more diffuse anomalous regions. However, hydrogen and nitrogen anomalies are not correlated and D enrichments are not preferentially associated with isotopically primitive IDPs. Pre-solar silicate grains in the IDPs show a variety of isotopic compositions that are similar to the oxygen isotopic compositions of pre-solar silicate and oxide grains from primitive meteorites. Most of the grains have isotopic ratios consistent with origins from red giant or asymptotic giant branch stars. Pre-solar silicate abundances in the isotopically primitive IDPs are significantly higher than in most primitive meteorites, a characteristic that emphasizes the primitive nature of IDPs.

Citation

Floss C, FJ Stadermann, JP Bradley, ZR Dai, S Bajt, G Graham, and AS Lea. 2006. "Identification of Isotopically Primitive Interplanetary Dust Particles: A NanoSIMS Isotopic Imaging Study." *Geochimica et Cosmochimica Acta* 70:2371-2399.

Optimum Conductivity in Oriented $[Ce_{0.89}Sm_{0.11}]O_{2-x}$ Thin Films Grown by Oxygen-Plasma-Assisted Molecular Beam Epitaxy

ZQ Yu,[(a)] LV Saraf,[(b)] OA Marina,[(c)] CM Wang,[(b)] MH Engelhard,[(b)] V Shutthanandan,[(b)] P Nachimuthu,[(b)] DE McCready,[(b)] and S. Thevuthasan[(b)]

(a) Nanjing Normal University, Nanjing, China

(b) W.R. Wiley Environmental Molecular Sciences Laboratory, Richland, Washington

(c) Pacific Northwest National Laboratory, Richland, Washington

Investigations in alternative and clean energy technology have become essential to reduce the dependence on more traditional energy resources. Solid oxide fuel cells (SOFC) provide such clean energy without hazardous by-products. The research described in this highlight is motivated by the use of epitaxial Sm:CeO_2 as a potential electrolyte material in SOFC. In this study, we have observed high conductivity values in epitaxial Sm:CeO_2 films.

Development of electrolyte materials that possess high oxygen ion conductance at relatively low temperatures is essential to increase the efficiency and lifetime of SOFC. Lower operating temperatures would make SOFCs more cost efficient and could facilitate their use in broader applications. At lower operating temperatures, SOFCs could also avoid many

undesirable interfacial reactions between electrodes and electrolyte materials. In this study, we used molecular-beam epitaxy, which enables precise growth control, to grow SOFC electrolyte layers. Oriented electrolyte layers, such as Sm:CeO_2, can potentially provide higher conductivity through a reduction in grain-boundary density, thus avoiding the unnecessary scattering across a layer. Sm:CeO_2 films were grown on single crystal c-Al_2O_3 in a dual-chamber, ultrahigh-vacuum system equipped with an electron cyclotron resonance oxygen plasma source.

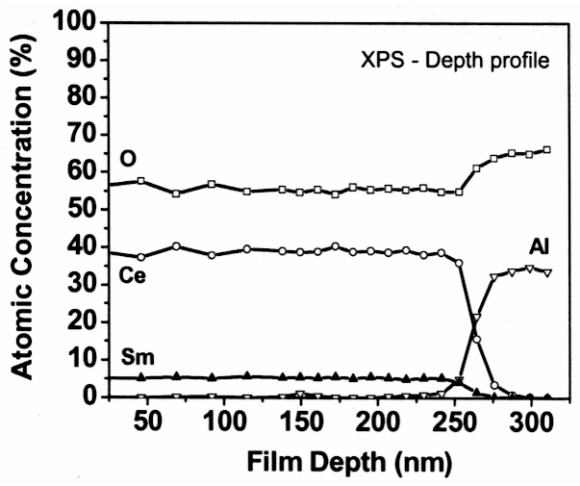

Figure 1. The XPS depth profile of 5 atom% Sm:CeO_2 film on c-Al_2O_3. A uniform samarium concentration throughout the film with surface oxygen enhancement can also be seen in the data.

After the surface plasma cleaning at 600°C, films were grown at simultaneous growth rates of 0.2 and 0.01 nm/s for cesium and samarium, respectively, in an oxygen partial pressure of ~2.0×10^{5} Torr and at a substrate temperature of 650°C. Cesium (99.98 percent purity) and samarium (99.98 percent purity) were evaporated from an e-bam source and an effusion cell, respectively. The growth rates of the films were monitored by quartz crystal oscillators (QCOs). The *in situ* film growth was monitored using reflection high-energy electron diffraction.

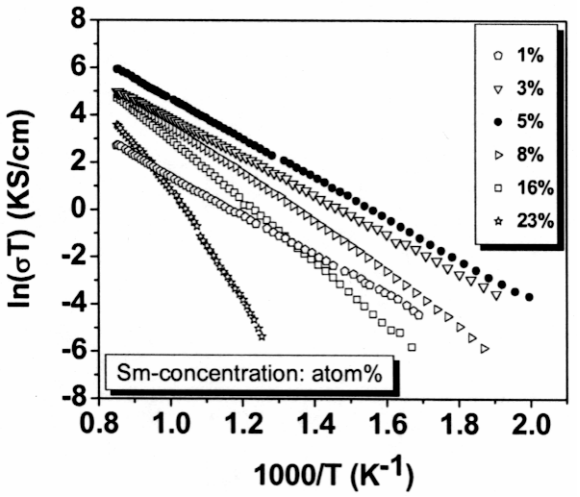

Figure 2. Arrhenius plots of Sm:CeO_2 films with various samarium atomic concentrations in the measurement temperature range of 500 to 900°C.

X-ray photoelectron spectroscopy (XPS) depth profiles give excellent overviews of the atomic elemental concentrations of cesium, samarium, oxygen, and aluminum as a function of film depth. Figure 1 shows the XPS depth profile in the case of 5 atom% Sm:CeO_2 film. A uniform samarium concentration as a function of film depth was noted, and $Ce_{0.89}Sm_{0.11}O_{2-x}$ was determined to be the stoichiometry of the film. In addition, a fairly sharp interface between Sm:CeO_2 and Al_2O_3 was also realized from the spectra. Four-probe conductivity measurements were done on Sm:CeO_2 films with samarium concentration in the range of 1 to 23 atom%. Figure 2 shows Arrhenius plots of Sm:CeO_2 films with various samarium atomic concentrations in the measurement temperature range of 500 to 900°C. The figure shows that film with a 5 atom% samarium concentration shows maximum conductivity compared to other doping concentrations. We concluded that a loss of (111) orientation enhances the grain boundary scattering, thereby reducing the conductivity. However, our

observed conductivity of 0.04 $S.cm^{-1}$ at 600°C is one of the highest conductivities observed in these materials. The activation energy E_a, derived from the slope of the Arrhenius plot, is observed at 0.86 eV for the as-grown films. Typically lower activation energy refers to lower barrier for the oxygen transport throughout the Sm:CeO_2 crystal.

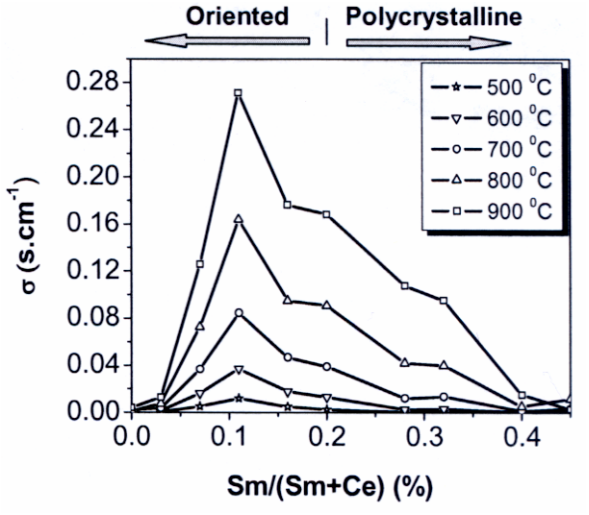

Figure 3. The conductivity of Sm:CeO_2 as a function of samarium concentration in the range of 1–23 atom% at measurement temperatures from 500 to 900°C. At all measurement temperatures, highest conductivity is seen at 5 atom% samarium concentration.

Figure 3 shows the conductivity of Sm:CeO_2 as a function of Sm/ (Sm+Ce) for the samarium concentration range of 1 to 23 atom%. The variation in conductivity as a function of temperature with different samarium concentrations is seen to get narrower at lower and higher samarium concentrations. The dopant saturation is likely to cause narrower conductivity variation at the higher samarium concentrations end, whereas limited dopant incorporation is primarily responsible for narrower variation at lower samarium concentrations.

Thermal Oxidation of Aluminum Nitride Powder

Z Gu,[a] JH Edgar,[a] CM Wang,[b] and DS Coffey[c]

(a) Kansas State University, Manhattan, Kansas

(b) W.R. Wiley Environmental Molecular Sciences Laboratory, Richland, Washington

(c) Pacific Northwest National Laboratory, Richland, Washington

The goal of this study was to determine and compare the oxidation behavior of two types of aluminum nitride (AlN) powder with different morphology and particle sizes. The kinetics of oxidation, the properties of the formed aluminum oxide layer, and the morphology change before and after oxidation were studied in detail using a combination of x-ray diffraction analysis and tunneling electron microscopy.

Aluminum nitride has a good thermal stability (melting point >2750°C), high thermal conductivity (3.2 W/cm·K) and electrical resistivity (>4 × 10^8 ohm·cm), and a low dielectric constant (9 at 1 MHz) and coefficient of thermal expansion (4.03-6.09 × 10^{-6}/K). Therefore, AlN has been widely used in the electronic and optoelectronic areas. Oxygen, a common impurity in AlN, has a detrimental effect on its properties: it reduces the lattice parameters of AlN and remarkably decreases its thermal conductivity. Therefore, understanding how oxygen enters the AlN lattice constitutes an important step for understanding the oxidation process. For example, a native oxide film of 5 to

10 nm in thickness is obtained following exposing AlN in air for 24 hours at room temperature. This initial oxide layer is protective and prevents further oxidation.

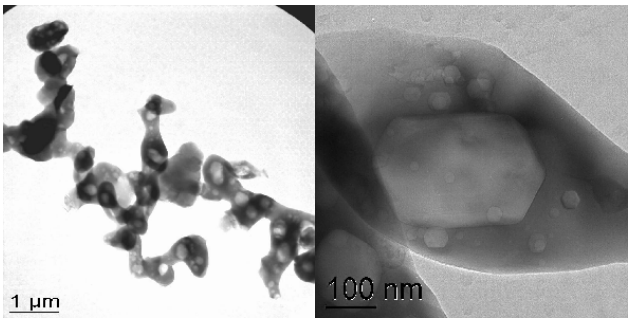

Figure 1. Transmission electron microscopy images of oxidized AlN particles, revealing a pore trapped in a particle.

In general, three sequential steps occur during the thermal oxidation of most materials, one of which may be the rate-limiting step. First, the oxidant (typically oxygen or water vapor) transports in the gas phase to the oxide surface. Second, the oxidant diffuses through the oxide layer to the substrate/oxide interface. Third, and finally, the oxidation reaction occurs at the interface. The diffusion process in the gas phase is usually very fast compared to the other two steps, thus it is insignificant in determining the overall growth kinetics. Initially, when the oxide layer is thin, the oxidant quickly transports through the oxide to the interface to sustain the chemical reaction, hence the whole process is controlled by the interfacial reaction. As the oxide layer thickness increases, the diffusion of the oxidant through the oxide layer slows and becomes the rate-limiting step in the overall process. The thermal oxidation of silicon is a typical example of the three-step process. However, in the thermal oxidation of AlN, which is governed by the overall reaction $2AlN + 1.5O_2 \leftrightarrow Al_2O_3 + N_2$, the out-diffusion of product gas nitrogen through the oxide film and the removal of nitrogen away from the oxide surface are two additional steps that are not involved in the oxidation of silicon. The latter step is usually rapid and is not a rate-controlling step.

Two types of AlN powder were oxidized in flowing oxygen over the temperature range from 800 to 1150°C. For a Type-A AlN powder (average agglomerated particle size 1.8 µm), oxidation began above 900°C after 6 hours and was almost complete at 1050°C, but only for 30 minutes. Crystalline Al_2O_3 formed above 1050°C, while amorphous Al_2O_3 or oxynitrides formed at lower temperatures. The oxidation of Type-A AlN powder was a linear reaction over time between 800 and 1000°C, and the activation energy was 157.2 kJ/mol. These conditions indicated that an interfacial reaction governed the process. At temperatures higher than 1000°C (1050, 1100, and 1150°C), approximately 95 percent of the AlN was oxidized after only 30 minutes, and the conversion barely changed with further increases in the oxidation temperature or time. For a Type-B AlN powder (particle size 14.0 to 23 µm), oxidation became observable at 800°C after 6 hours, and the oxidation extent was higher than that of Type-A AlN powder at temperatures ranging from 800 to 1000°C. The oxidation kinetics changed from linear in the 800 to 900°C temperature range to parabolic in the 1000 to 1150°C range, suggesting that control of the process changed from interfacial reaction control to oxidant diffusion control. The complex oxidation difference observed between the two AlN powder types was probably caused by the different morphologies of the powders, and by their different particle sizes, particle-size distributions, and impurities. Figure 1 shows transmission electron microscopy images of oxidized AlN particles, revealing a pore trapped in a particle.

Oxidation of AlN powders, sintered polycrystalline substrates, and thin films has been extensively investigated. Abid et al. (1986) found that AlN powder was resistant to oxidation in air up to ~1000°C. For AlN powder heated to 1000°C, an unidentified phase was detected by reflection high-energy electron diffraction, possibly an oxide or oxynitride. At 1200°C, the AlN was completely transformed to α-Al_2O_3. However, no differences were reported for the oxidation of AlN powders with different particle sizes. Brown et al. (1998) observed a linear weight increase of AlN powder over time when heated in air at 850°C. The activation energy was calculated to be 271 kJ/mol. At temperatures above 850°C, the weight change increased parabolically, and the activation energy was 423 kJ/mol, which agreed well with the 459 kJ/mol experimental value for the diffusion of oxygen through polycrystalline Al_2O_3. X-ray diffraction, scanning electron microscopy, and infrared spectroscopy were employed by Ramanthan et al. (1995) to study the oxidation behavior of AlN powder at temperatures in the 900 to 1150°C range. An initial linear kinetic regime with activation energies of 197 and 270 kJ/mol was observed. A poorly crystalline spinel-type aluminum oxynitride formed at 900°C. This phase was transformed into α-alumina crystallites at higher temperatures. The oxide morphology changed from a fine-grained and coherent structure at 950°C to a porous fissured structure at 1150°C.

In addition to oxidation temperature and time, the condition of the original AlN powder is crucial in determining the thermal oxidation behavior. Particle size and impurity concentration are two important parameters in describing AlN powder. The surface-area-to-volume ratio of small particles is typically much higher than that of large particles, leaving more surface area exposed per mass. Thus, small particles are expected to oxidize faster than larger particles. The effect of particle size on the AlN oxidation rate was examined by Suryanarayana (1990). The initially rapid oxidation rate decreased over time for a fine AlN powder with a mean particle radius and standard deviation of 0.5 μm and 1.6, respectively. In contrast, the oxidation rate was almost constant with time for a coarse powder with a mean particle radius and a standard deviation of 3.1 μm and 2.1, respectively. Highly doped silicon substrates oxidize more rapidly than lightly doped silicon wafers, and the difference in reaction rates is greater at lower temperatures or for thinner oxides. One possible explanation is that oxidation requires volume expansion that can be provided by the consumption of vacancies at the silicon/silicon dioxide interface.

An article describing this research was published in the July 2006 edition the *Journal of the American Ceramic Society* (Gu et al. 2006).

Citations

Abid A, R Bensalem, and BJ Shealy. 1986. "The Thermal Stability of AlN." *Journal of Materials Science* 21(4):1301-1304.

Brown AL and MG Norton. 1998. "Oxidation Kinetics of AlN Powder." *Journal of Materials Science* 17(18):1519-1522.

Gu Z, JH Edgar, CM Wang, and DW Coffey. 2006. "Thermal Oxidation of Aluminum Nitride Powder." *Journal of the American Ceramic Society* 89(7)2167-2171.

Ramanathan S, R Bhat, DD Upadhyaya, and SK Roy. 1995. "Oxidation Behavior of Aluminum Nitride Powder." *British Ceramic Transactions* 94(2):74-78.

Suryanarayana D. 1990. "Oxidation Kinetics of Aluminum Nitride Powders." *Journal of the American Ceramic Society* 73(4):1108-1110.

Study of Hydrogen Stability in Low-K Dielectric Films by Ion Beam Techniques

Y Zhang,[a] L Saraf,[a] V Shutthanandan,[a] KD Hughes,[a] R Kuan,[b] and S Thevuthasan[a]

(a) W.R. Environmental Molecular Sciences Laboratory, Richland, Washington
(b) Texas Instruments Incorporated, Dallas, Texas

With shrinking device geometries into the 65-nm technology node, a transition to low-k dielectrics becomes increasingly attractive. Negative bias temperature instability, which is associated with hydrogen migration at elevated temperatures, becomes the main degradation mechanism of concern for conductivity breakdown in semiconductor devices. The possibility of hydrogen release during each stage of the fabrication process is, therefore, of great interest to the understanding of device reliability. In this study, various low-k dielectric films were subjected to thermal annealing in a nitrogen atmosphere at temperatures that are generally used when fabricating devices. Rutherford backscattering spectrometry (RBS) and elastic recoil detection analysis (ERDA) were used to investigate composition changes and hydrogen redistribution of the dielectric films.

In interlayer dielectric (ILD) applications, plasma-enhanced tetraethylorthosilicate (PETEOS) films have been used to achieve better step coverage, especially for submicron gap spaces. With addition of phosphorus dopants during the deposition, phosphorus-doped silicon glass (PSG) films become viscous at elevated temperatures and respond to surface tension forces and the rounding of sharp corners, which is extremely useful in forming uniform doping inside gaps with high aspect ratios.

Furthermore, PSG films have an alkali ion-gettering capability, which makes it well suited for use as a passivation layer. In this project, the composition changes of the PETEOS and PSG films before and after annealing at 400°C for 2 hours were studied by RBS. The RBS spectra along with the simulated spectra are presented in Figures 1(a) and 2(a). In addition, hydrogen stability was

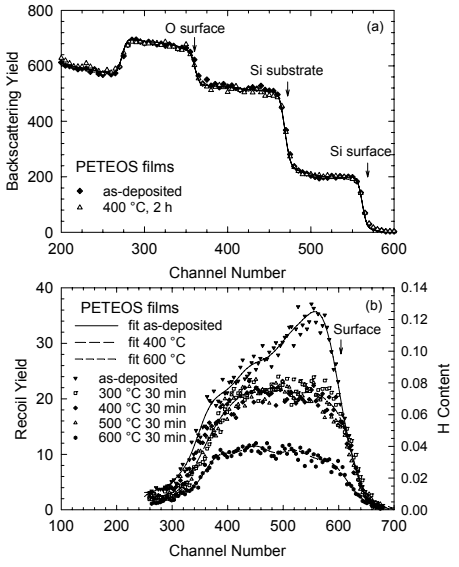

Figure 1. (a) RBS spectra of PETEOS films before and after 400°C for 2 hours; (b) ERDA spectra of the as-deposited PETEOS film and the films that are subjected to thermal treatments.

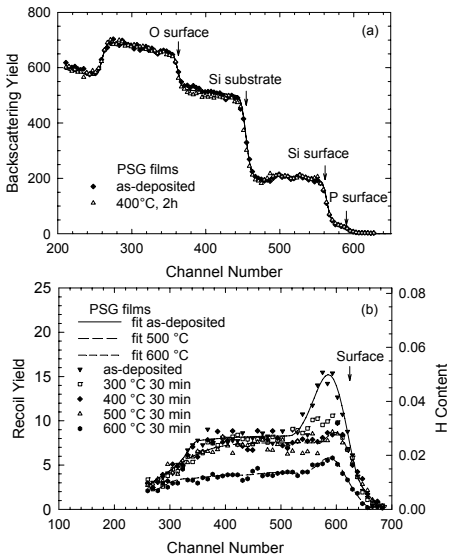

Figure 2. (a) RBS spectra of PSG films before and after 400°C for 2h. (b) ERDA spectra of the as-deposited and annealed PSG films.

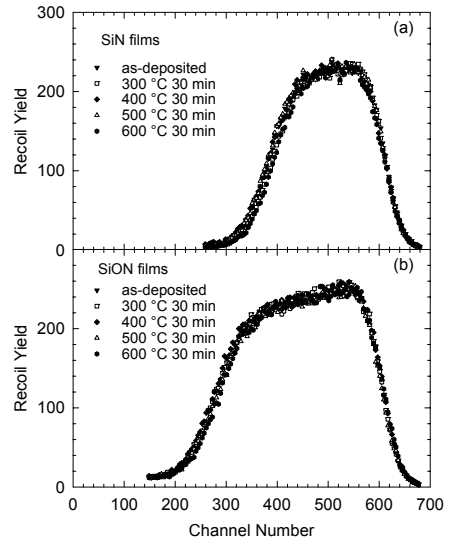

Figure 3. ERDA spectra of the as-deposited film and annealed (a) SiN films and (b) SiON films.

investigated by measuring the total hydrogen in the films using conventional ERDA after the heat treatments up to 600°C, as shown in Figures 1(b) and 2(b). In the figures, higher hydrogen concentrations are observed in the surface regions of as-deposited PETEOS and PSG films. In the as-deposited films, the hydrogen concen-tration in the surface region consists of hydrogen from the films and from the hydrocarbon contamination on the film surfaces. After heat treatment up to 400°C for 2 hours, the main structures of both films are preserved. Significant hydrogen reductions at both the PETEOS and the PSG sample surfaces are observed after annealing at 300°C. Although the PETEOS films show some hydrogen reduction in the bulk of the film after this annealing, reduction of hydrogen is less significant in the bulk of the PSG films, indicating the existence of weakly bound hydrogen compounds in the bulk of the PETEOS films. After annealing at 400 and 500°C, no significant hydrogen reduction is observed in both films, and hydrogen is more uniformly distributed in the films, approximately 7.5 percent in the PETEOS films and 2.5 percent in the PSG films. As the annealing temperature increases to 600°C, both the PETEOS and PSG films decompose with significant hydrogen releases, and a SiO_2 film begins to form.

Silicon nitride (SiN) is a widely used dielectric material in very large-scale integration fabrication because of its impermeability to most impurities, such as a diffusion barrier to moisture, or as a selective oxidation mask to prevent oxygen from penetrating into the silicon underlayer. Silicon oxynitride (SiON) films, in which the composition changes continuously from oxide to nitride by varying gas flow during plasma-enhanced chemical vapor deposition, demonstrate improved stability and better cracking resistance with low film stress. Thus, SiON films are considered to be unique materials for intermetal-level dielectric and final passivation layers. The SiN and SiON films are thermally stable up to 600°C annealing, (Figure 3). No hydrogen redistribution or structural changes are observed within the measurement uncertainties.

To further decrease the dielectric constant of the ILD layers as the device dimension decreases to sub-100-nm fields, introducing nanoscale pores into the dielectrics is an effective approach for meeting ultra-low-k demand. Among various porous low-k materials, organosilicate glass (OSG) films are promising candidates as ILD materials for high-performance interconnects. The OSG films used in this study were carbon-doped, low-k material with incorporated organic groups (e.g., -CH_3). No change was observed after heat treatment up to 400°C for 2 hours. ERDA results indicate that hydrogen bonds are stable up to 500°C for 30 minutes, as shown in Figure 4. However, release of hydrogen from the film during 600°C annealing is evident.

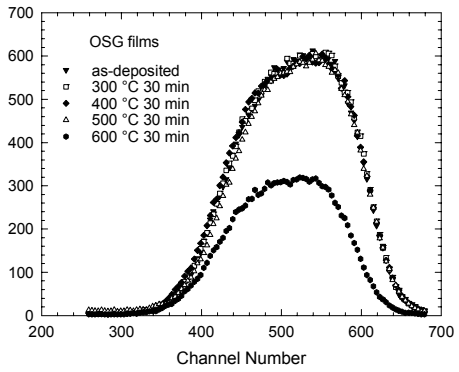

Figure 4. ERDA spectra of the as-deposited and thermally treated OSG films.

In this project, we investigated the stability of low-k dielectric films subjected to heat treatment up to 600°C. The results indicate that there is a significant hydrogen release from the surface region of the PETEOS and PSG films at 300°C and insignificant hydrogen releases in the temperature range from above 300°C to 500°C. The films start to decompose by releasing hydrogen at 600°C and form SiO_2. The SiN and SiON films are stable after heat treatment at 600°C for 30 minutes. Similar to the PETEOS and PSG films, the OSG films are stable up to 500°C and then break down at 600°C.

User Projects

Field Emission SEM of Anode Supported YSZ Fuel Cells Poisoned by Cr

SP Simner, J Kim, Pacific Northwest National Laboratory, Richland, Washington

MH Engelhard, Environmental Molecular Sciences Laboratory, Richland, Washington

Surface and Interface Study of Contacts to Carbon-based Films

TC Droubay, Pacific Northwest National Laboratory, Richland, Washington

LM Porter, PB Kulkarni, Carnegie Mellon University, Pittsburgh, Pennsylvania

Determination of the Catalytic Properties of Metal Coated Nanowires

AD Lalonde, MG Norton, Washington State University, Pullman, Washington

Novel Electrochemical Process for Treatment of Perchlorate

G Liu, Pacific Northwest National Laboratory, Richland, Washington

The Study of Atomic Gold Clusters in Polyaniline

AH Saheb, M Josowicz, JA Janata, Georgia Institute of Technology, Georgia Tech Research Corporation, Atlanta, Georgia

Surface Characterization of Ambient Ultrafine Particles

EL Bullock, AM Johansen, C Thomas-Bradley, Central Washington University, Ellensburg, Washington

Stability of H Species in Various Dielectric Films used in Advanced Microelectronic Fabrication

YR Kuan, Texas Instruments Incorporated, Dallas, Texas

Routine SEM Analysis of Lysed *Bacillus* Spores

CL Warner, CJ Bruckner-Lea, Pacific Northwest National Laboratory, Richland, Washington

B Arey, Environmental Molecular Sciences Laboratory, Richland, Washington

Microscopy of Hanford Tank Sludge

EC Buck, Pacific Northwest National Laboratory, Richland, Washington

Electron Microscopy Investigation of Bacterial Outer Membrane Vesicles

MJ Kuehn, Duke University, Durham, North Carolina

Surface Area and Porosity Analyses of Mesoporous Thin Films and Powders

RD Champion, S Li, AR Courtney, Pacific Northwest National Laboratory, Richland, Washington

SEM Investigation of Thermal Barrier Coatings and ODS Alloys

GJ Grant, Pacific Northwest National Laboratory, Richland, Washington

B Arey, Environmental Molecular Sciences Laboratory, Richland, Washington

TEM Study on SOFC Interconnects

Z Yang, Pacific Northwest National Laboratory, Richland, Washington

An Experimental and Data Analysis Investigation into the Trapped Gases and Non-ice Material in the Surfaces of the Outer Planets Icy Satellites

CA Hibbitts, Johns Hopkins University, Laurel, Maryland

Physical Characterization of Defects in ZnO Diluted Magnetic Semiconductors

KR Kittilstved, DR Gamelin, University of Washington, Seattle, Washington

Investigation of Oxygen Diffusion in Single Crystal STO Films Grown on Si

ZJ Yu, Freescale Semiconductor Inc., Tempe, Maryland

Characterization of Mesoporous SiO_2 Particles for the Characterization of Non-ideal Sorption Behavior

DR Yonge, DL Washington, Washington State University, Pullman, Washington

Electrochemical Sensors and Biosensors for Environmental and Health Monitoring

J Xu, Nanjing University, Nanjing, China

Electrochemical Detection of Lead in Saliva

W Yantasee, A Cinson, D Choi, Pacific Northwest National Laboratory, Richland, Washington

Kn Hongsirikarn, Tn Sangvanich, K Pattamakomsan, Chulalongkorn University, Bangkok, Thailand

Molecular Beam Epitaxy Growth of Strontium Cobaltite

AJ Anderson, South Dakota School of Mines and Technology, Rapid City, South Dakota

Trace Metal Composition of Cobalt

JB Cliff, Pacific Northwest National Laboratory, Richland, Washington

A Combinatorial Sputtering Approach to Magnetic Properties Modification of FeCoB

DP Pappas, National Institute of Standards and Technology, Boulder, Colorado

RR Owings, Applied Materials, Boise, Idaho

Controlling the Thermal and Non-Thermal Reactivities of Metal Oxide Structures Through Nanoscaling - Controlling Reactivities of Metal Oxide Structures

MA Henderson, KM Rosso, NI Iordanova, SA Chambers, M Dupuis, AG Joly, JE Jaffe, G Xiong, Rn Shao, Pacific Northwest National Laboratory, Richland, Washington

IV Lyubinetsky, KM Beck, Environmental Molecular Sciences Laboratory, Richland, Washington

MS Gutowski, Heriot-Watt University, Edinburgh, United Kingdom

X-ray Photoelectron Diffraction of MgO(111)-(1x1)

RA Plass, Sandia National Laboratory, Milwaukee, Wisconsin

M Gajdardziska-Josifovska, University of Wisconsin, Milwaukee, Milwaukee, Wisconsin

Electrochemical and TEM Characterization of Metal Nanoparticles Deposited in Carbon Nanotubes

CM Wai, Y Lin, University of Idaho, Moscow, Idaho

Chemical Characterization of Sub-micrometer Mineral Phases in Extraterrestrial Materials that have Previously been Characterized by NanoSIMS Isotope Imaging

FJ Stadermann, C Floss, Washington University in St. Louis, St. Louis, Missouri

T Yada, Institute of Astronomy and Astrophysics, Academia Sinica, Taipei, Taiwan, Province Of China

Chemically-selective Sensor Film Characterization

Z Wang, Pacific Northwest National Laboratory, Richland, Washington

WR Heineman, N Pantelic, University of Cincinnati, Cincinnati, Ohio

Advanced Electrode Concepts for CdZnTe Radiation Detectors

CE Seifert, G Dunham, Pacific Northwest National Laboratory, Richland, Washington

Advanced Electrode Concepts for CdZnTe Radiation Detectors

CE Seifert, G Dunham, Pacific Northwest National Laboratory, Richland, Washington

MH Engelhard, Environmental Molecular Sciences Laboratory, Richland, Washington

Energetic Ion Studies of Key Future Technological Materials

MI Laitinen, University of Jyvaskyla, Jyvaskyla, Finland

HJ Whitlow, V Touboltsev, University of Jyväskylä, Jyväskylä, Finland

Investigation of the Surface Characteristics of Chemically Modified Natural Fibers

LS Fifield, JD Holbery, Pacific Northwest National Laboratory, Richland, Washington

X-ray Powder Diffraction Study of Fe_2O_3-Mn_2O_3 Phase Diagram

JV Crum, Pacific Northwest National Laboratory, Richland, Washington

Mesopore Uniformity and Hydrothermal Stability of Silica Thin Films for High Permeabilty Applications

RE Williford, Pacific Northwest National Laboratory, Richland, Washington

Stability of Ceria and Other Nanoparticles

Sn Kuchibhatla, S Seal, D Bera, University of Central Florida, Orlando, Florida

KH Pecher, Pacific Northwest National Laboratory, Richland, Washington

DR Baer, Environmental Molecular Sciences Laboratory, Richland, Washington

Nano-porous TiO_2 Ceramics

A Bandyopadhyay, Washington State University, Pullman, Washington

Novel Micro-manipulation Methods for Radioactive Particle Isolation and Characterization with Energy-filtered Electron Microscopy

EC Buck, BK McNamara, Pacific Northwest National Laboratory, Richland, Washington

A Dohnalkova, Environmental Molecular Sciences Laboratory, Richland, Washington

SEM/EDS of Solid Oxide Fuel Cell Seal Materials

JS Vetrano, Pacific Northwest National Laboratory, Richland, Washington

B Arey, Environmental Molecular Sciences Laboratory, Richland, Washington

Thermogravimetric Analysis of Organometallic Compounds and Semiconductor/Metal Nanoparticles

MG Warner, Pacific Northwest National Laboratory, Richland, Washington

XPS Studies of Self-Assembling Monolayers

BJ Tarasevich, Pacific Northwest National Laboratory, Richland, Washington

Understanding the Properties of Oxide and Metal Nanostructures

S Sivarajah, K Ahilan, University of Jaffna, Jaffna, Sri Lanka

Electroactive Materials for Anion Separation -- Technetium from Nitrate

TL Hubler, SD Rassat, Pacific Northwest National Laboratory, Richland, Washington

Spectroelectrochemical Sensor for Technetium Applicable to the Vadose Zone (PNNL Scope # 30948 Bryan/Hubler EMSP)

AS Del Negro, TL Hubler, SA Bryan, Z Wang, Pacific Northwest National Laboratory, Richland, Washington

WR Heineman, CJ Seliskar, University of Cincinnati, Cincinnati, Ohio

Surface Migration of Additives in Polymers

LA Archer, VS Minnikanti, Cornell University, Ithaca, New York

Characterization of Functional Nanoscale Materials for Vapor Sensing

SP Garland, University of California, Davis, Redding, California

CL Aardahl, RS Addleman, LS Fifield, F Zheng, DL Baldwin, On Reid, Pacific Northwest National Laboratory, Richland, Washington

B Arey, Environmental Molecular Sciences Laboratory, Richland, Washington

Oxidation State of Technetium Electrodeposited on Platinum

MD Engelmann, Pacific Northwest National Laboratory, Richland, Washington

AR Coatings

WD Bennett, DC Stewart, CC Bonham, DW Matson, Pacific Northwest National Laboratory, Richland, Washington

Characterization of Oxide Nanoparticles

L Wang, Pacific Northwest National Laboratory, Richland, Washington

XPS Study of CeO_2 and $CeZrO_2$

L Wang, Pacific Northwest National Laboratory, Richland, Washington

S Azad, UCAR Carbon Company Inc., Parma, Ohio

Novel Biosensor Based on Nanomaterials

G Liu, Y Lin, Pacific Northwest National Laboratory, Richland, Washington

B Arey, Environmental Molecular Sciences Laboratory, Richland, Washington

Surface Analysis of Functional Carbons

Y Shin, Pacific Northwest National Laboratory, Richland, Washington

Ion-Beam Synthesis of Materials for Hydrogen Storage

W Jiang, Pacific Northwest National Laboratory, Richland, Washington

***In situ* FTIR Studies of Alumina in a Hydrogen Environment: a Study of Hydrogen Chemistry within Ceramics**

AC Stowe, RH Jones, CH Henager, J Szanyi, Pacific Northwest National Laboratory, Richland, Washington

Steam Reforming of Bio-mass

H Roh, Pacific Northwest National Laboratory, Richland, Washington

Homogeneous Precipitation of Cerium Dioxide Nanoparticles

C Tseng, Oregon State University, Corvallis, Oregon

EC Buck, Pacific Northwest National Laboratory, Richland, Washington

Nanocrystalline MoS_2 Catalysts

WJ Shaw, J Franz, Pacific Northwest National Laboratory, Richland, Washington

Determination of Nanoporous Material Oxidation States

DM Wellman, AJ Karkamkar, Zn Hontz, En Richards, Pacific Northwest National Laboratory, Richland, Washington

Characterization of Pure and Doped ZnO Nanoclusters

J Antony, Y Qiang, University of Idaho, Moscow, Idaho

Z Wang, Pacific Northwest National Laboratory, Richland, Washington

Study of Some Specific Inclusions in a Garnet Matrix Using High Resolution Transmission Electron Microscopy (HRTEM)

MJ Guinel, MG Norton, Washington State University, Pullman, Washington

TOF-SIMS and Auger Studies of Ozone Oxidation of Unsaturated Self Assembled Monolayers on Silicon Surfaces

BJ Finlayson-Pitts, TM McIntire, University of California, Irvine, Irvine, California

PL Gassman, Environmental Molecular Sciences Laboratory, Richland, Washington

Preparation, Characterization and Application of Chemical Modified Electrodes

X Cui, Fudan University, Shanghai, China

XPS Analysis of Fabric Chars to Determine the Phosphorous - Nitrogen Synergism in Flame Retardants

S Gaan, S Gang, University of California, Davis, Davis, California

Image Iron Oxide Nanoparticles

GR Holtom, Environmental Molecular Sciences Laboratory, Richland, Washington

Stabilization of Polar Oxide Interfaces: Integrated Experimental and Theoretical Studies of Atomic Structure and Electronic Properties

S Cheung, Pacific Northwest National Laboratory, Richland, Washington

M Gajdardziska-Josifovska, University of Wisconsin, Milwaukee, Milwaukee, Wisconsin

Ion Beam Characterization of Nanocomposite Tribological Coatings

RJ Smith, PE Gannon, Montana State University, Bozeman, Montana

Surface Texture of Zircon Grains from the Sierra Madera Impact Structure, West Texas

SA Huson, MC Pope, Washington State University, Pullman, Washington

Thrust 4: Model Hematite Thin Films and Bacterial Iron Reduction

TC Droubay, Z Wang, L Shi, BH Lower, Pacific Northwest National Laboratory, Richland, Washington

TW Wietsma, Environmental Molecular Sciences Laboratory, Richland, Washington

Characterization of Manganese Cobalt Oxides Using XPS

G Xia, Pacific Northwest National Laboratory, Richland, Washington

Molecularly Organized Nanostructural Materials

Y Shin, Gn Exarhos, CF Windisch, AR Teodoro-Dier, Pacific Northwest National Laboratory, Richland, Washington

B Arey, Environmental Molecular Sciences Laboratory, Richland, Washington

Measurements of Aerosol Composition by Aircraft during the 2005 Marine Stratus Experiment

PH Daum, Brookhaven National Laboratory, Upton, New York

Nuclear Reaction Analysis of Biotite Minerals

CV Ramana, En Essene, University of Michigan, Ann Arbor, Michigan

Determination of Cause of Bloating in Ti Pellets

NL Canfield

Pacific Northwest National Laboratory, Richland, Washington

Preparation of ZnO Thin Films by MOCVD

KR Kittilstved, DR Gamelin, University of Washington, Seattle, Washington

Investigation of Structural Properties of Oxide and Nitride Nanowires

MC Johnson, Lawrence Berkeley National Laboratory, University of California, Berkeley, Berkeley, California

Characterization of GaN/InGaN/GaN Thin Film Structures

F Ohuchi, E Venkatasubramanian, K Poochinda, University of Washington, Seattle, Washington

Compositionally Graded Co and Cr Doped TiO_2 Rutile for Optimum Thermoelectric Power

L Saraf, V Shutthanandan, Environmental Molecular Sciences Laboratory, Richland, Washington

A Yamamoto, AIST, Ibaraki, Japan

F Ohuchi, S Iwanaga, University of Washington, Seattle, Washington

Electron Microscopy of Single-walled Carbon Nanotubes during Growth on CoMo Bimetallic Catalysts

N Sakulchaicharoen, DE Resasco, University of Oklahoma, Norman, Oklahoma

Aerosol Sampling

PC Gray, Los Alamos National Laboratory, los alamos, New Mexico

Catalytic Ammonia Oxidation

GE Fryxell, Pacific Northwest National Laboratory, Richland, Washington

Structural Analysis of Kinetically Stabilized Core-Shell Nanoparticles

B Eichhorn, University of Maryland, College Park, Maryland

Analysis of Nanoparticulates

EW Hoppe, Pacific Northwest National Laboratory, Richland, Washington

SEM Analysis of Rotating Drum Impactor Filter Strips for Biological Species

ML Alexander, Environmental Molecular Sciences Laboratory, Richland, Washington

Adhesion of Polymer Sphere to Modified Natural Fiber via AFM

JD Holbery, Pacific Northwest National Laboratory, Richland, Washington

Collaborative Water Initiative Project on Stabilization of Water Treatment Residuals

SV Burnside, JK Shaw, WP Ela, University of Arizona, Tucson, Arizona

Systematical Study of Novel Nano-magnetic Materials

D Li, Y Liu, X Wang, Alfred University, Alfred, New York

J Helfer, Biophan Technologies, Inc., West Henrietta, New York

Functionally Graded Brake Materials

EV Stephens, Pacific Northwest National Laboratory, Richland, Washington

Determination P-dopant Concentration in Wide Band Gap SnO_2 Semiconductor, using RBS technique

SB Rananavare, A Chaparadza, Portland State University, Portland, Oregon

Fabrication of Microconduits

G Dunham, Pacific Northwest National Laboratory, Richland, Washington

Low Temperature Si Device Fabrication

B Arey, Environmental Molecular Sciences Laboratory, Richland, Washington

C Shih, ST Dunham, H Guo. University of Washington, Seattle, Washington

The Microstructural Influence on Fatigue Crack Growth in Rene 88DT

E Sackmann, KO Findley, Washington State University, Pullman, Washington

Characterizing Size, Morphology, and Mechanical Properties of Superalloy Carbides

J Hutchinson, KO Findley, JD Yeager, Washington State University, Pullman, Washington

Analysis of the Composition of Cu Films

R Johnson, DP Field, Washington State University, Pullman, Washington

Design and Synthesis of Tailored Band-Gap SiGe(C) Detectors

CH Henager, Pacific Northwest National Laboratory, Richland, Washington

M Elfman, Lund Institute of Technology, Lund, Sweden

Depth Profiles of Isotopic Oxygen in Cerium Oxide Catalysts

DA Berry, National Energy Technology - Laboratory, Morgantown, West Virginia

Surface Characterization of Granular Iron from Cores of an In Situ Permeable Reactive Barrier

PG Tratnyek, Oregon Health Sciences University/Oregon Graduate Institute, Beaverton, Oregon

PIXE Elements Analysis of Carbon Nanosheets

M Zhu, BC Holloway, College of William and Mary, Williamsburg, Virginia

Norovirus TEM Proposal, Straub

C Nickerson, K Honer Zu Bentrup, Tulane University, New Orleans, Louisiana

TM Straub, Pacific Northwest National Laboratory, Richland, Washington

CP Gerba, University of Arizona, Tucson, Arizona

B Arey, Environmental Molecular Sciences Laboratory, Richland, Washington

B Mayer, Arizona State University, Tempe, Arizona

Rhenium and Technetium Uptake by Iron-Based Materials

KM Krupka, Pacific Northwest National Laboratory, Richland, Washington

B Arey, Environmental Molecular Sciences Laboratory, Richland, Washington

Friction stir processing TiB_2 into the Surface of Class 40 Grey Cast Iron to Improve the Wear Resistance

U Ramasubramanian, South Dakota School of Mines and Technology, Rapid City, South Dakota

GJ Grant, Pacific Northwest National Laboratory, Richland, Washington

Profilometry Studies of Printed Electrode Films for Fuel Cell Applications

CF Windisch, Pacific Northwest National Laboratory, Richland, Washington

Cost Effective Ultra-thin Palladium Based Membrane for Hydrogen Separation and Purification

Y Peng, Innovatek, Inc., Richland, Washington

High Resolution TEM Images and Electron Diffractions for Gold Nanotubes/Nanorods and Metal Vanadate Nanotubes/Nanorods

Y Wang, G Cao, University of Washington, Seattle, Washington

Nickel Coating of Polymer Microbeads

RM Ozanich, Pacific Northwest National Laboratory, Richland, Washington

Electron Microscopy Imaging of Cyanobacteria *Synechcystis sp*

C Gassman, Columbia Basin College, Pasco, Washington

A Dohnalkova, B Arey, Environmental Molecular Sciences Laboratory, Richland, Washington

Electron Energy Loss in Radiation Detection

B Cannon, EC Buck, Pacific Northwest National Laboratory, Richland, Washington

C Wang, Environmental Molecular Sciences Laboratory, Richland, Washington

Electron Microscopy of Novel Metal-Transforming Bacteria from Extreme Environments

TS Magnuson, Idaho State University, Pocatello, Idaho

Characterization of Tungsten Carbide Synthesized by Controlled Template Method

J Kwak, Pacific Northwest National Laboratory, Richland, Washington

B Arey, Environmental Molecular Sciences Laboratory, Richland, Washington

Investigation Cellulose Phase Change and Interaction with Other Molecules by DSC

H Zhao, Pacific Northwest National Laboratory, Richland, Washington

Determination of the Silica Polymorphs Thermally Grown on Silicon Carbide as a Function of Temperature and Time using X-ray Photoelectron Spectroscopy (XPS)

MJ Guinel, MG Norton, Washington State University, Pullman, Washington

Study of the Ferromagnetic Activation in ZnO Diluted Magnetic Semiconductors

CR Johnson, KR Kittilstved, DR Gamelin, University of Washington, Seattle, Washington

Transient Kinetics Experiments for Studying Catalytic Reactions for H_2 Production

Y Yang, RS Disselkamp, Pacific Northwest National Laboratory, Richland, Washington

CT Campbell, RJ Chimentao, L Cameron, IM Jensen, University of Washington, Seattle, Washington

Scanning Electron Microscopy of *Corynebacterium glutamicum*

H Yukawa, Research Institute of Innovative Technology for the Earth, Kizu, Japan

Ecophysiological Investigation of Cyanobacteria using Controlled Cultivation

YA Gorby, KM Rosso, EA Hill, Pacific Northwest National Laboratory, Richland, Washington

B Arey, Environmental Molecular Sciences Laboratory, Richland, Washington

Optical Properties of Ag Nanoparticles Embedded in Polymer Matrices

TD Pounds, MG Norton, Washington State University, Pullman, Washington

Controlling Field Emission from HV Structures

M Zhu, BC Holloway, College of William and Mary, Williamsburg, Virginia

Structural Characterization of Complex Electrodes

SA Towne, JD Holbery, Pacific Northwest National Laboratory, Richland, Washington

Characterization of Oxide Based Diodes

GS Herman, WF Stickle, Hewlett-Packard Company, Corvallis, Oregon

SEM-EDS Elemental Mapping of Weymouth Soils

KJ Cantrell, Pacific Northwest National Laboratory, Richland, Washington

B Arey, Environmental Molecular Sciences Laboratory, Richland, Washington

Segregation on Annealed R-Cut Sapphire Surfaces

SB Rivers, RJ Lad, University of Maine, Orono, Maine

Nanoengineered Electrochemical Sensor for Mixed Wastes

J Wang, Pacific Northwest National Laboratory, Richland, Washington

Structure of the *Shewanella* Cell Surface

AL Neal, University of Georgia, Aiken, South Carolina

Epitaxial Growth and Properties of Candidate Diluted Magnetic Oxide Semiconductors - Chemistry and Physics of Ceramic Surfaces

TC Kaspar, SA Chambers, TC Droubay, S Heald, AR Teodoro-Dier, Pacific Northwest National Laboratory, Richland, Washington

Evaporative Co-deposition of Fluoride Materials

DW Matson, Pacific Northwest National Laboratory, Richland, Washington

B Arey, Environmental Molecular Sciences Laboratory, Richland, Washington

Microscopic Analysis of Carbon-based Nanomaterials

Y Shin, Pacific Northwest National Laboratory, Richland, Washington

B Arey, Environmental Molecular Sciences Laboratory, Richland, Washington

Measurement of Band Gap, Band Offset, and Thickness for Ultra-thin SiO_2, SiON and High-k Films on Si

Z Chen, CB Samantaray, University of Kentucky, Lexington, Kentucky

High-resolution Ion Scattering Studies of Nano-scale Oxide Films and Thermal Stability of Oxide-semiconductor Interfaces

S Ramanathan, C Chang, Harvard University, Cambridge, Massachusetts

Evaluation of SIMS for Location of Bacterial Spores and to Source Growth Media and Geographic Location

JB Cliff, Pacific Northwest National Laboratory, Richland, Washington

Test Mass Characterization for Precision Gravitational Tests

CD Hoyle, TS Cook, EG Adelberger, University of Washington, Seattle, Washington

Synthesis of Sub-micron Cuprous Oxide Films on a Silicon Nitride Membrane for Study using Time-resolved X-ray Techniques

PB Hillyard, Stanford University, Stanford, California

KJ Gaffney, Stanford Synchrotron Radiation Laboratory, Menlo Park, California

Investigation of Electron Emission from Nano-structures

AY Wong, J Chen, University of California, Los Angeles, Los Angeles, California

R Wang, Nonlinear Ion Dynamics, LLC, Van Nuys, California

Molecular Beam Scattering Measurements on Anatase TiO_2(001) and Rutile TiO_2(110)

U Burghaus, North Dakota State University, Fargo, North Dakota

Fabrication of Si Templates for the Construction of Monolithic Multi-Electrospray Emitters

RT Kelly, K Tang, R Smith, Pacific Northwest National Laboratory, Richland, Washington

Olefins by High-Intensity Oxidation

Y Wang, D Kim, R Dagle, J Hu, X Wang, Pacific Northwest National Laboratory, Richland, Washington

Hydrogen Production

Y Wang, D Kim, J Hu, X Wang, CM Fischer, R Kou, Pacific Northwest National Laboratory, Richland, Washington

Integrated Automated Analyzer for Groundwater Monitoring

Y Lin, G Liu, J Wang, W Yantasee, Pacific Northwest National Laboratory, Richland, Washington

MH Engelhard, Environmental Molecular Sciences Laboratory, Richland, Washington

Klin Phosphoric Acid Process

T Hart, Pacific Northwest National Laboratory, Richland, Washington

Mechanisms of Sulfur Poisoning of NOx Adsorber Materials

CH Peden, Pacific Northwest National Laboratory, Richland, Washington

MH Engelhard, Environmental Molecular Sciences Laboratory, Richland, Washington

Microstructural Examination of SOFC Materials Development

DS Gelles, Pacific Northwest National Laboratory, Richland, Washington

Trace Impurities in Graphite Crucible used for Advanced Detector Materials Synthesis

JB Cliff, M Bliss, Pacific Northwest National Laboratory, Richland, Washington

High Resolution TEM Analysis of $CuInS_2$ Nanoparticles and XRD analysis of $CuInS_2$ Thin Films

JJ Pak, L Lau, JS Gardner, Idaho State University, Pocatello, Idaho

Site Specific Valence Above and Below the Verwey Transition in Magnetite

TC Droubay, TC Kaspar, SA Chambers, Pacific Northwest National Laboratory, Richland, Washington

JO Cross, Argonne National Laboratory, Argonne, Illinois

X-ray Analysis of Quantum Well Films

PM Martin, Pacific Northwest National Laboratory, Richland, Washington

TGA Analysis of Synthesized Organic Components of Self-assembled Monolayers on Mesoporous Silica

RJ Wiacek, RS Addleman, An Cinson, J Davidson, Pacific Northwest National Laboratory, Richland, Washington

The Use of FESEM

X Zhou, Pacific Northwest National Laboratory, Richland, Washington

Ion Beam Modification of Advanced Titanium Alloys

KO Findley, CP Norby, Washington State University, Pullman, Washington

Center of Excellence for Chemical Hydrogen Storage

T Autrey, Pacific Northwest National Laboratory, Richland, Washington

Technetium (Tc) Reduction by Chemically and Biologically Reduced Smectite Clay

H Dong, Miami University, Oxford, Ohio

Applications of Nanostructured Materials and Electrodes in Electrochemical Sensors and Fuel Cell

X Cui, Fudan University, Shanghai, China

Computational and Experimental Nanoparticle Dosimetry for Nanomaterial Safety

JG Teeguarden, Pacific Northwest National Laboratory, Richland, Washington

Micro-fabrication of Miniaturized Solid Oxide Fuel Cell (SOFC) on Silicon Chip

P Singh, O Marina, Pacific Northwest National Laboratory, Richland, Washington

L Saraf, T Thevuthasan, Environmental Molecular Sciences Laboratory, Richland, Washington

Development of Wet Chemical Etching Methods to Create Chalcogenide Glass Film Structures

A Qiao, N Anheier, K Krishnaswami, Pacific Northwest National Laboratory, Richland, Washington

Trace Signatures in Particles

JB Cliff, Pacific Northwest National Laboratory, Richland, Washington

High Surface Area Nanocrystalline SiC Material Analysis

Y Wang, J Kwak, J Hu, D Howe, Pacific Northwest National Laboratory, Richland, Washington

DM Ginosar, Idaho National Engineering and Environmental Laboratory (INEEL), Idaho Falls, Idaho

Characterization of Microstructure and Composition of Magnetostrictive Nanobars for Bio-sensor Application

S Li, Z Cheng, Auburn University, Auburn, Alabama

Fundamental Investigations of Heterogeneous Catalysis Using Isotopic Transient Kinetic Analysis -(Scope 90001)

RS Disselkamp, J Szanyi, J Kwak, Y Yang, Pacific Northwest National Laboratory, Richland, Washington

CT Campbell, University of Washington, Seattle, Washington

C Mims, University of Toronto, Toronto, Ontario, Canada

Surface-Modified Iron Oxide Nanoparticle Characterization by Transmission Electron Microscopy

JW Gunn, N Bhattarai, M Zhang, University of Washington, Seattle, Washington

Development of a Catalyst for the Steam Reformation of JP-10

R Dagle, Pacific Northwest National Laboratory, Richland, Washington

D Nguyen, Energia Technologies, INC, Castro Valley, California

Spectroscopic Study of the Bioactivity of Nanoparticles by Exposure to Human Lung Cells

D Dutta, BM Moudgil, University of Florida, Gainsville, Florida

SK Sundaram, Pacific Northwest National Laboratory, Richland, Washington

X-ray Photoelectron Spectroscopy and Expert Consulting on Thermal Stabilization of Multi-component Inorganic Oxide Materials

GE Spanner, LR Pederson, Pacific Northwest National Laboratory, Richland, Washington

MH Engelhard, Environmental Molecular Sciences Laboratory, Richland, Washington

H Gysling, AirFlow Catalysts Systems, Inc., Rochester, New York

Examine the Compositions of the Black Sands in Northern Oregon

JS Young, David Heil Associates Corporation, Portland, Oregon

Equilibrium-induced Decomposition of Nitrates on a NOx Storage/Reduction Catalyst

WS Epling, University of Waterloo, Waterloo, Ontario, Canada

X-ray Photoemission Study of Graphite

S Azad, UCAR Carbon Company Inc., Parma, Ohio

The *in vivo* Localization and Interactions between Structural Components of the *Shewanella oneidensis* MR-1 Metal Reducing System by High Resolution Transmission Electron Microscopy

MJ Marshall, Pacific Northwest National Laboratory, Richland, Washington

A Dohnalkova, Environmental Molecular Sciences Laboratory, Richland, Washington

The Biogeochemical Mechanisms Controlling Reduced Radionuclide Particle Formation Properties and Stability

MJ Marshall, Pacific Northwest National Laboratory, Richland, Washington

Radionuclide Reduction by *Anaeromyxabacter dehalogenans*

FE Loeffler, Georgia Institute of Technology, Georgia Tech Research Corporation, Atlanta, Georgia

Chromium Diffusion Kinetics in Nano-ceria and Doped Ceria Coatings: An UCF-PNNL Collaboration

S Seal, RK Thanneeru, Sn Kuchibhatla, University of Central Florida, orlando, Florida

Spectroscopic and Microscopic Characterization of Graphite

S Azad, UCAR Carbon Company Inc., Parma, Ohio

Non-destructive SEM-based Analysis of Complex Functional Structures in Insects: Development of Tools for Rapid Species Diagnosis in Tropical Biodiversity Surveys

NO Pellmyr, University of Idaho, Moscow, Idaho

High-resolution Interfacial Studies of Nano-scale Oxide Films

S Ramanathan, Harvard University, Cambridge, Massachusetts

Effects of Temperature and Time (130 Years) on Surface Charges and Chemical Properties of Black Carbon

C Cheng, J Lehmann, BT Nguyen, Cornell University, Ithaca, New York

Molecular Beam Scattering Measurements on Anatase TiO_2(001) and Rutile TiO_2(110)

U Burghaus, North Dakota State University, Fargo, North Dakota

Characterization of Novel DNA/Semiconductor Nanoconjugates

F Zhou, Dn Jiang, California State University, Los Angeles, Los Angeles, California

Fundamental Investigations of Heterogeneous Catalysis Using Isotopic Transient Kinetic Analysis

S Chuang, University of Akron, Akron, Ohio

RS Disselkamp, Pacific Northwest National Laboratory, Richland, Washington

MG White, Georgia Institute of Technology, Georgia Tech Research Corporation, Atlanta, Georgia

CT Campbell, University of Washington, Seattle, Washington

J Goodwin, Clemson University, Clemson, South Carolina

C Mims, University of Toronto, Toronto, Ontario, Canada

Characterization of High Surface Area Tungsten Carbide Synthesized by Templated Synthesis Methods Electrocalytic Applications

J Kwak, Pacific Northwest National Laboratory, Richland, Washington

Post Growth Analysis of Compositionally Graded InGaN Grown with MOCVD

F Ohuchi, E Venkatasubramanian, K Poochinda, C Lu, University of Washington, Seattle, Washington

Compositionally Graded V_2O_5 for Improved Thermoelectric Power

A Yamamoto, AIST, Ibaraki, Japan

F Ohuchi, S Iwanaga, University of Washington, Seattle, Washington

Novel Catalytic Materials for the Hydrodesulfurization and Water-Gas Shift Processes

ME Bussell, Western Washington University, Bellingham, Washington

Amorphous Semiconductor Analysis using Ion Beam Tools

CH Henager, Pacific Northwest National Laboratory, Richland, Washington

Fundamental Studies of Nitrogen Oxide Surface Chemistry: A Model System Approach

Y Kim, Hanbat National University (formerly Taejon National University of Technology), Taejon, Korea South, Republic Of

J Szanyi, CH Peden, Pacific Northwest National Laboratory, Richland, Washington

C Yi, Texas A&M University, College Station, Texas

IV Lyubinetsky, Environmental Molecular Sciences Laboratory, Richland, Washington

Post Growth Analysis of GaN and InGaN Grown with MOCVD

E Venkatasubramanian, K Poochinda, T Chen, University of Washington, Seattle, Washington

Hydrogen Materials Compatibility Studies

CH Henager, JD Holbery, Pacific Northwest National Laboratory, Richland, Washington

Model Oxide Defects with Vicinally Stepped NiO(100) Substrates

MA Langell, University of Nebraska, Lincoln, Nebraska

MBE Growth and Properties of Model TiO_2 Surfaces for Fundamental Studies of Heterogeneous Photocatalysis

SA Chambers, R Shao, MA Henderson, Pacific Northwest National Laboratory, Richland, Washington

C Wang, DE McCready, Y Du, Environmental Molecular Sciences Laboratory, Richland, Washington

MBE Growth and Properties of N-doped TiO_2 for Enhanced Visible Light Absorption and Water Splitting

SA Chambers, S Cheung, S Heald, MA Henderson, Pacific Northwest National Laboratory, Richland, Washington

J Rodriguez, Brookhaven National Laboratory, Upton, New York

C Wang, DE McCready, V Shutthanandan, Environmental Molecular Sciences Laboratory, Richland, Washington

C Fadley, Lawrence Berkeley National Laboratory, Richland, West Virginia

Epitaxial Growth and Properties of Magnetically Doped ZnO Prepared by Pulsed Laser Deposition of Nanoparticle Targets

SA Chambers, TC Droubay, TC Kaspar, Pacific Northwest National Laboratory, Richland, Washington

KM Whitaker, CR Johnson, KR Kittilstved, DR Gamelin, SA Santangelo, PI Archer, University of Washington, Seattle, Washington

Real-time FTIR Measurements of Fe-oxide Transformation in Presence of Dissimilatory Fe-reducing Bacteria

GG Geesey, Montana State University, Bozeman, Montana

TC Droubay, Pacific Northwest National Laboratory, Richland, Washington

Visualization of a Pd-Au{100} Catalyst: a Scanning Tunneling Microscopy Study

P Han, DW Goodman, Texas A&M University, College Station, Tennessee

Directed Self-assembly of Metal Oxide Island Nanostructures

JF Groves, University of Virginia, Charlottesville, Virginia

Y Du, DR Baer, Environmental Molecular Sciences Laboratory, Richland, Washington

Structure-Property Relationships in Thin Film Energy Conversion Materials and Coatings

DW Matson, PE Burrows, LC Olsen, PM Martin, ME Gross, WD Bennett, CC Bonham, G Graff, ES Mast, SN Kundu, AB Padmaperuma, LS Sapochak, Pacific Northwest National Laboratory, Richland, Washington

Nerve Agent Detection Using Enzyme-Coated Nanowires

Y Koo, S Lee, Inha University, Incheon, Korea South, Republic Of

J Kim, Pacific Northwest National Laboratory, Richland, Washington

S Kim, S Nair, Pennsylvania State University, University Park, Pennsylvania

J Lee, Chosun University, Gwangju, Korea South, Republic Of

Elemental Characterization of Ionizer Filaments for Thermal Ionization Mass Spectrometry (TIMS)

JB Cliff, MD Engelmann, Pacific Northwest National Laboratory, Richland, Washington

Molecular-level Understanding of Transport and Optic Properties of Doped Oxide Nanoclusters

Y Qiang, J Antony, M Faheem, University of Idaho, Moscow, Idaho

Molecular Level Construction of Functional Surfaces

SM Gorun, New Jersey Institute of Technology, Newark, New Jersey

Selective Heterogeneous Catalysis

LS Fifield, T Bays, Pacific Northwest National Laboratory, Richland, Washington

Early Transition Metal Oxides as Catalysts: Crossing Scales from Clusters to Single Crystals to Functioning Materials

E Iglesia, University of California, Berkeley, Berkeley, California

CH Peden, Jn Hu, J Kwak, J liu, Y Wang, X She, G Xia, D Kim, JF White, Pacific Northwest National Laboratory, Richland, Washington

VM Lebarbier, University of New Mexico, Albuquerque, New Mexico

DA Dixon, University of Alabama, Tuscaloosa, Tuscaloosa, Alabama

NOx Adsorber Materials: Fundamental Studies, and Investigations of Sulfur Poisoning and Thermal Deactivation

CH Peden, RS Disselkamp, D Kim, J Kwak, J Szanyi, RG Tonkyn, CM Verrier, D Tran, J Male, Pacific Northwest National Laboratory, Richland, Washington

Metal-induced Crystallization via Sputtering Deposition on Flexible Substrates and its Applications

ST Dunham, C Shih, H Guo, University of Washington, Seattle, Washington

Development of Room Temperature Ferromagnetism in Wide-band-gap Oxide Semiconductor Nanostructures

A Punnoose, Boise State University, Boise, Idaho

Chemistry of Outer Solar System Materials

TB McCord, GB Hansen, University of Washington, Seattle, Washington

An Experimental and Data Analysis Investigation into the Trapped Gases and Non-ice Material in the Surfaces of the Outer Planets Icy Satellites and Our Moon

CA Hibbitts, Johns Hopkins University, Laurel, Maryland

J Szanyi, Pacific Northwest National Laboratory, Richland, Washington

Crystal Perfection in Cadmium Zinc Telluride Radiation Detectors

MB Toloczko, M Bliss, Z Wang, Pacific Northwest National Laboratory, Richland, Washington

Photochemical Studies on N-doped TiO_2 Single Crystals - Fundamental Investigations of Water Splitting on Model TiO_2

VH Lam, University of Central Florida, Orlando, Florida

MA Henderson, SA Chambers, S Cheung, R Shao, SC Andrews, Pacific Northwest National Laboratory, Richland, Washington

IV Lyubinetsky, T Thevuthasan, P Nachimuthu, Y Du, Environmental Molecular Sciences Laboratory, Richland, Washington

Biomineralology and Ultrastructure of Neutrophilic Iron-oxidizing Bacteria

KJ Edwards, University of Southern California, Los Angeles, California

CS Chan, Woods Hole Oceanographic Institution, Woods Hole, Massachusetts

Study of Thermal Decomposition of Polyester Fibers Treated with Phosphorus Flame Retardants

S Gaan, G Sun, University of California, Davis, Davis, California

Enhanced Ionic Conductivity of Samaria Doped Ceria Thin Films through Tailoring the Dopant Concentration and Microstructures

L Bauder, S Michael, Pacific Northwest National Laboratory, Richland, Washington

Z Jaquish, Environmental Molecular Sciences Laboratory, Richland, Washington

Z Yu, Nanjing Normal University, Nanjing, China

Cryo-EM Investigations of Interfacial Bacterial Extracellular Polymeric Substance (EPS) in Vanadium Interactions

MJ Marshall, Pacific Northwest National Laboratory, Richland, Washington

The Role of PdZn Alloy Formation and Particle Size on the Selectivity for Steam Reforming of Methanol

AM Karim, A Datye, T Conant, University of New Mexico, Albuquerque, New Mexico

Characterization of Chemistry and Physics at Metal-Polythiophene and Metal-Carbon Interfaces

LM Porter, KA Singh, PB Kulkarni, Carnegie Mellon University, Pittsburgh, Pennsylvania

Model System Surface Science Approach to Study Photochemistry at Adsorbate-substrate Interfaces: The Trimethyl Acetate, Silver, Titania System

MA Henderson, Z Dohnalek, SC Andrews, Pacific Northwest National Laboratory, Richland, Washington

IV Lyubinetsky, Environmental Molecular Sciences Laboratory, Richland, Washington

JM White, University of Texas at Austin, Austin, Texas

Bone Growth on Tailored Biomimetic Surfaces

MI Laitinen, University of Jyvaskyla, Jyvaskyla, Finland

HJ Whitlow, University of Jyväskylä, University of Jyväskylä, Finland

Defects and Defect Processes in Ceramics

WJ Weber, W Jiang, I Bae, BD Milbrath, Pacific Northwest National Laboratory, Richland, Washington

L Boatner, Oak Ridge National Laboratory, Oak Ridge, Tennessee

Catalytic and Optical Properties of Surface Attached and Matrix Embedded Quantum Dots

G Duscher, North Carolina State University, Raleigh, North Carolina

Electron Energy Loss in Radiation Detection Materials

B Cannon, AJ Carman, Pacific Northwest National Laboratory, Richland, Washington

P Nachimuthu, C Wang, Environmental Molecular Sciences Laboratory, Richland, Washington

Thin Film Electrolyte/Electrode Development and Enhanced Ionic Transport in Miniaturized Solid Oxide Fuel Cells on Silicon Chips

P Singh, O Marina, Pacific Northwest National Laboratory, Richland, Washington

Surface and Bulk Characterization of Ambient Ultrafine Particles

EL Bullock, AM Johansen, C Thomas-Bradley, Central Washington University, Ellensburg, Washington

Surface Characterization of Calcium Phosphates

WJ Shaw, BJ Tarasevich, Pacific Northwest National Laboratory, Richland, Washington

Mixed Oxide Films for Gas Sensing and Photo-catalytic Applications

KR Padmanabhan, Wayne State University, Detroit, Michigan

Spin Electronic Phenomena in Magnetically Doped Perovskites and Complex Oxide Interfaces

TC Kaspar, SA Chambers, TC Droubay, Pacific Northwest National Laboratory, Richland, Washington

C Wang, DE McCready, V Shutthanandan, T Thevuthasan, Environmental Molecular Sciences Laboratory, Richland, Washington

Materials for Automotive Sensor Development

GW Coffey, Pacific Northwest National Laboratory, Richland, Washington

Toward Preparation and Operando Characterization of Nanostructured Heterogeneous Photocatalysts

Y Shin, GE Fryxell, XS Li, RE Williford, K Parker, Pacific Northwest National Laboratory, Richland, Washington

Near Real-time Alkene Sensor for Atmospheric Aerosol Chemistry Monitoring

JW Grate, Pacific Northwest National Laboratory, Richland, Washington

R Shekarriz, MicroEnergy Technologies, Inc., Portland, Oregon

Design of Micro-cantilever Actuators for Measuring Surface Tension of Sub Microliter Volumes Applied Towards Monitoring Interfacial Processes

DW Britt, BA Henrie, Utah State University, Logan, Utah

Characterization of Mixed Monolayers with X-ray Photoelectron Spectroscopy (XPS)

L Liu, M Yan, Portland State University, Portland, Oregon

D Hu, Pacific Northwest National Laboratory, Richland, Washington

The Thickness Measurement of Electrolyte Cast on Mylar Film

S Hong, VL Sprenkle, Pacific Northwest National Laboratory, Richland, Washington

Thin Film X-ray Diffraction Studies of Calcium Phosphate Films and XPS Studies of Self-Assembling Monolayers

BJ Tarasevich, Pacific Northwest National Laboratory, Richland, Washington

Reforming of Hydrocarbons on Solid Oxide Fuel Cell Anodes

JJ Strohm, X Wang, DL King, Y Wang, Pacific Northwest National Laboratory, Richland, Washington

Structural and Chemical Properties of Catalysts

ME Bussell, AW Burns, Western Washington University, Bellingham, Washington

Characterizations of NiAu Bimetallic Butane Steam Reforming Catalyst

Y Chin, Pacific Northwest National Laboratory, Richland, Washington

Structure and Composition of Electrochemically Active Mixed Metal Oxides

LR Pederson, CD Nguyen, Z Nie, X Zhou, Pacific Northwest National Laboratory, Richland, Washington

Response of Radiation Detector Materials to Ions

BD Milbrath, Pacific Northwest National Laboratory, Richland, Washington

Low Angle X-ray Characterization of Catalyst Porosity

XS Li, Pacific Northwest National Laboratory, Richland, Washington

Mechanisms of Environment-Assisted Degradation in Reactor Materials

JS Vetrano, S Bruemmer, Pacific Northwest National Laboratory, Richland, Washington

Gold Hollow Nanostructures: Synthesis and Optical Properties

X Lu, Y Xia, University of Washington, Seattle, Washington

Characterization of Metal Nanoparticles for Optimization of Process Parameters to Support Synthesis of Well-defined Carbon Nanotubes

LS Fifield, Pacific Northwest National Laboratory, Richland, Washington

A Gupta, VB Mikheev, Battelle Columbus, Columbus, Ohio

Cellular Internalization Studies of Semiconductor Nanoparticles in Bacteria

A Punnoose, MR Kongara, Boise State University, Boise, Idaho

Understanding Particle Generation and the Risk of Occupational Exposure and Environmental Release of Nanoparticles During Processing of Nanocomposite Materials

DJ Gaspar, TJ Johnson, Z Wang, Pacific Northwest National Laboratory, Richland, Washington

MG Yost, University of Washington, Seattle, Washington

A Gupta, ML Clark, Battelle Columbus, Richland, Washington

Evaluation of Multicomponent Porous Oxide Films

XS Li, Pacific Northwest National Laboratory, Richland, Washington

B Arey, Environmental Molecular Sciences Laboratory, Richland, Washington

Spectroscopy and Microscopy of Doped TiO_2 Nanocrystalline Materials

DR Gamelin, JD Bryan, NS Norberg, KM Whitaker. University of Washington, Seattle, Washington

Investigation of Oxidation State of Elements in Natural Brannerites

MX Colella, Australian Nuclear Science & Technology Org. (ANSTO), Lucas heights, Australia

EC Buck, Pacific Northwest National Laboratory, Richland, Washington

Nondestructive Carbon Nanotube Modification of Tailored Functionality

LS Fifield, CL Aardahl, Pacific Northwest National Laboratory, Richland, Washington

J Li, University of Washington, Seattle, Washington

Investigating Electrochemical Properties, Composition and Oxidation States of Nanoparticles and Catalysts Using Electrochemistry and XPS

C Zhong, State University of New York at Binghamton, Binghamton, New York

Use of EMSL Scanning Microscopy Capabilities to Study Soil Mineral Weathering

Z Balogh, JT Dickinson, CK Keller, AL Espana, Washington State University, Pullman, Washington

SEM of Life Stages of Gall Wasps of the Family *Cynipidae*

JD DeMartini, Humboldt State University, Arcata, California

SEM Image Acquisition, X-ray Elemental Analysis

RM Ozanich, Pacific Northwest National Laboratory, Richland, Washington

Reaction Specificity of Nanoparticles in Solution

J Antony, Y Qiang, A Sharma, University of Idaho, Moscow, Idaho

RL Penn, C Chun, University of Minnesota, Minneapolis, New Mexico

M Dupuis, BD Kay, EJ Bylaska, JE Amonette, KH Pecher, Pacific Northwest National Laboratory, Richland, Washington

AA El-Azab, Florida State University, Tallahassee, Florida

DR Baer, MH Engelhard, TW Wietsma, C Wang, Environmental Molecular Sciences Laboratory, Richland, Washington

PG Tratnyek, Oregon Health Sciences University/Oregon Graduate Institute, Beaverton, Oregon

Experimental and Theoretical Studies of Reaction Pathways for the Breakdown of Chlorinated Hydrocarbon Molecules by Metal and Metal Oxide Nanoparticles

J Antony, Y Qiang, A Sharma, University of Idaho, Moscow, Idaho

RL Penn, University of Minnesota, Minneapolis, Minnesota

S Kuchibhatla, University of Central Florida, Orlando, Florida

M Dupuis, BD Kay, EJ Bylaska, JE Amonette, Z Dohnalek, Pacific Northwest National Laboratory, Richland, Washington

AA El-Azab, Florida State University, Tallahassee, Florida

RK Kukkadapu, DR Baer, MH Engelhard, TW Wietsma, C Wang, PL Gassman, Environmental Molecular Sciences Laboratory, Richland, Washington

GS Parkinson, University of Warwick, Coventry, United Kingdom

PG Tratnyek, J Nurmi, V Sarathy, Oregon Health Sciences University/Oregon Graduate Institute, Beaverton, Oregon

Experimental Measurements of the Band Offsets of Epitaxial Silicon on $LaAlO_3$ Single Crystals

SA Chambers, JR Williams, Pacific Northwest National Laboratory, Richland, Washington

LF Edge, DG Schlom, V Vaithyanathan, Pennsylvania State University, University Park, Pennsylvania

Using Ni-ion Irradiation for the Development of Advanced Materials for the Next Generation Nuclear Reactor

TR Allen, University of Wisconsin-Madison, Madison, Wisconsin

J Gan, Argonne National Laboratory - West, Idaho Falls, Idaho

Characterization of Mn Oxidation State with Electron Energy Loss Spectroscopy

EC Buck, Pacific Northwest National Laboratory, Richland, Washington

Characterization and Method Development for Back-end of the Line Wafer Processing Concepts

AJ Carman, TS Zemanian, CR Yonker, JL Fulton, DW Matson, BJ Tarasevich, RJ Orth, GE Fryxell, AH Zacher, Pacific Northwest National Laboratory, Richland, Washington

B Arey, Environmental Molecular Sciences Laboratory, Richland, Washington

DJ Hymes, LAM Research Corporation, Fremont, California

Oxidation Studies of Coatings for Interconnect Plates in Solid Oxide Fuel Cells

RJ Smith, AN Kayani, PE Gannon, Montana State University, Bozeman, Montana

CV Ramana, University of Michigan, Ann Arbor, Michigan

Metallurgical Characterization of Coatings Deposited by Electrospark Deposition

J Keegan, WE Wood, GA Tewksbury, Portland State University, Portland, Oregon

Solid Phase Transformations in the Hanford Sediments Treated with Al-rich, Hyperalkaline and Saline Solutions

NP Qafoku, Pacific Northwest National Laboratory, Richland, Washington

Immobilized Enzymes for Bioremediation and Biosensing - Armored Enzyme Nanoparticles for Remediation of Subsurface Contaminants

X Zhao, University of Minnesota, Minneapolis, Minnesota

S Lee, Inha University, Incheon, Korea South, Republic Of

H Jia, University of Akron, Akron, Ohio

J Kim, JW Grate, Pacific Northwest National Laboratory, Richland, Washington

TE Herricks, University of Washington, Seattle, Washington

J Lee, C Lee, K Min, S Chung, H Na, Seoul National University, Seoul, Korea South, Republic Of

M Kim, J Youn, Korea Advanced Institute of Science and Technology (KAIST), Daejeon, Korea South, Republic Of

S Nair, Pennsylvania State University, University Park, Pennsylvania

H Ahn, BS Kim, Chungbuk National University, Chungbuk, Korea South, Republic Of

B Kim, Gwangju Institute of Science and Technology (GIST), Gwangju, Korea South, Republic Of

S Jun, Dongguk University, Seoul, Korea South, Republic Of

Immobilized Enzymes for Bioremediation and Biosensing

MB Fischback, Washington State University, Pullman, Washington

S Lee, Y Koo, Inha University, Nam-gu Incheon, Korea South, Republic Of

H Jia, University of Akron, Akron, Ohio

J Kim, JW Grate, Pacific Northwest National Laboratory, Richland, Washington

TE Herricks, University of Washington, Seattle, Washington

J Lee, C Lee, K Min, S Chung, H Na, Seoul National University, Seoul, Korea South, Republic Of

M Kim, J Youn, K Kwon, S Shin, Korea Advanced Institute of Science and Technology (KAIST), Daejeon, Korea South, Republic Of

S Nair, Pennsylvania State University, University Park, Pennsylvania

H Ahn, BS Kim, Chungbuk National University, Chungbuk, Korea South, Republic Of

B Kim, Gwangju Institute of Science and Technology (GIST), Gwangju, Korea South, Republic Of

J Lee, Chosun University, Gwangju, Korea South, Republic Of

Environmental Scanning Electron Microscopic Analysis of Gas Hydrate and Hydrate-Bearing Sediments

BP McGrail, Pacific Northwest National Laboratory, Richland, Washington

JS Young, David Heil Associates Corporation, Portland, Oregon

SEM on Electrode Surface/Electrode Preparation and Testing

W Yantasee, Pacific Northwest National Laboratory, Richland, Washington

The Measurements for Nano-tip'ID

R Zhao, Environmental Molecular Sciences Laboratory, Richland, Washington

Modified Carbon Supports for Aqueous Phase Catalysis--Applications for the Conversion of Glucose and Fermentation Products to Value-Added Chemicals

GE Fryxell, JF White, JG Frye, Pacific Northwest National Laboratory, Richland, Washington

SEM and SIMS Analysis of Organic Semiconductor Films Grown using Liquid Crystal Solvents

DL Patrick, FS Wilkinson, Western Washington University, Bellingham, Washington

Characterization of Heat Treated Silicon Carbide Specimens using Scanning Electron Microscopy

MJ Guinel, MG Norton, Washington State University, Pullman, Washington

High-resolution Transmission Electron Microscopic Evidences of Stacking Faults in Zeolitic Minerals Formed in Hanford Sediments Reacted with Simulated Tank Waste Solutions

Y Deng, Washington State University, Pullman, Washington

Nanoclusters, Nanomaterials and Nanotechnology - University of Washington/National Science Foundation

A Krishna, Louisiana State University, Baton Rouge, Louisiana

J Lee, C Qi, Portland State University, Beaverton, Oregon

AJ Anderson, WM Cross, T Engstrom, W Douglas, J Reams, W Weyer, A Vats, South Dakota School of Mines and Technology, Rapid City, South Dakota

J Antony, A Sharma, M Faheem, University of Idaho, Moscow, Idaho

MJ Guinel, AD Lalonde, L Wang, An Rogan, SR John, E Brown, M Al-khedher, C Dutton, J Hardy, M Pirzada, E Rude, H Singh, J Bevington, CD Fey, EH Khan, AA Lowell, P Rudenko, JL Schei, JL Serven, X Wang, MA Zaman, Washington State University, Pullman, Washington

FS Wilkinson, C Murphy, R Norwood, Western Washington University, Bellingham, Washington

S Maheswaran, University of Western Sydney, Nepean Australia, Kingswood,, Australia

JH Willet, University of Montana, Missoula, Montana

BA Henrie, Utah State University, Logan, Utah

Q Liu, AA El-Azab, Florida State University, Tallahassee, Florida

AP Kouprine, McGill University, Montreal, Quebec, Canada

DW Galipeau, South Dakota State University, Brookings, South Dakota

PB Kulkarni, KA Singh, Carnegie Mellon University, Pittsburgh, Pennsylvania

DR Baer, Environmental Molecular Sciences Laboratory, Richland, Washington

ML Cotten, P Davis, Pacific Lutheran University, Tacoma, Washington

DB Allred, SL Tait, LT Ngo, A Tankut, CM Lee, NT Nguyen, JH Wei, MT Zin, Jn Randall, R Ostermann, X Zheng, J Zou, H Sun, University of Washington, Seattle, Washington

G Seetharaman, Air Force Institute of Technology, Dayton, Ohio

L Wang, Washington State University Tri-Cities, Pullman, Washington

J Youngsman, Boise State University, Boise, Idaho

V Sarathy, S Sundara Rajan, Oregon Health Sciences University/Oregon Graduate Institute, Beaverton, Oregon

S Kothari, University of Tulsa, Tulsa, Oklahoma

J Hickey, University of South Florida, Tampa, Florida

KM Ball, PathScale Inc., Mountain View, California

X Cui, Fudan University, Shanghai, China

G Cushing, SP Ingole, DP Kulkarni, GP Lee, University of Alaska Fairbanks, Fairbanks, Alaska

M Burke, R Hendrickson, North Dakota State College of Science, Wahpenton, North Dakota

On-Line Determination of Selected Vapor-Phase Hoffmann List Compounds by PTR-MS

GM Anderson, Washington State University, Richland, Washington

DC-1 Molecular & Bio Imprinting

XS Li, Pacific Northwest National Laboratory, Richland, Washington

B Arey, Environmental Molecular Sciences Laboratory, Richland, Washington

Silicon Carbide Nanowires and Nanospings: Processing, Self-assembly, Characterization, and Properties

D Zhang, DN McIlroy, AI Alkhateeb, J Wei, YA Kranov, H Mahood, University of Idaho, Moscow, Idaho

AD Lalonde, Washington State University, Pullman, Washington

2-D Photonic Crystals Grown by Atomic Layer Deposition for Near IR and Visible Optoelectronics Applications

D Zhang, DN McIlroy, AI Alkhateeb, J Wei, YA Kranov, H Mahood, University of Idaho, Moscow, Idaho

AD Lalonde, Washington State University, Pullman, Washington

Mechanisms of Sulfur Poisoning of NOx Adsorber Materials

Y Chin, Pacific Northwest National Laboratory, Richland, Washington

Ion-Solid Interactions in Ceramics

WJ Weber, W Jiang, I Bae, Pacific Northwest National Laboratory, Richland, Washington

L Wang, University of Michigan, Ann Arbor, Michigan

P Nachimuthu, Environmental Molecular Sciences Laboratory, Richland, Washington

DK Shuh, Lawrence Berkeley National Laboratory, Berkeley, California

Materials and Methods for Multivariate Chemical Sensing

C Dutton, Washington State University, Richland, Washington

JW Grate, DL Baldwin, NC Anheier, MG Warner, AM Pierson, Pacific Northwest National Laboratory, Richland, Washington

AJ Tyler, Utah State University, Logan, Utah

Materials and Methods for Multivariate Chemical Sensing

C Dutton, Washington State University, Richland, Washington

JW Grate, DL Baldwin, NC Anheier, MG Warner, AM Pierson, RM Ozanich, B Hatchell, W Paxton, Pacific Northwest National Laboratory, Richland, Washington

AJ Tyler, Utah State University, Logan, Utah

Monolayer Protected Gold Nanoparticle Investigation and Characterization

JW Grate, BP Dockendorff, Pacific Northwest National Laboratory, Richland, Washington

LA Hughes, Southern Oregon University, Ashland, Oregon

Synthesis and Characterization of Novel Nanocrystalline Oxide Film Structures

Interface Controlled, Self-Assembled Oxide Quantum

CF Windisch, J Szanyi, Pacific Northwest National Laboratory, Richland, Washington

AA El-Azab, Florida State University, Tallahassee, Florida

JF Groves, RK Catalano, University of Virginia, Charlottesville, Virginia

Y Du, DR Baer, Environmental Molecular Sciences Laboratory, Richland, Washington

TEM Study of Carbon Nanotube Reinforced Polymer-Derived Ceramic Composites

L An, Y Wang, University of Central Florida, Orlando, Florida

PTR-MS Characterization of Carbon Nanotube Preconcentrators for Trace Chemical Signature Detection

F Zheng, Pacific Northwest National Laboratory, Richland, Washington

Characterization of Noble Metal Catalysts for Hydrogen Production and Purification in Fuel Cell Applications

S Chin, MD Amiridis, University of South Carolina, Columbia, South Carolina

Characterization Polymer Thin Films and Arrays

M Yan, J Ren, R Joshi, MB Harnish, Portland State University, Portland, Oregon

Y Chen, Oregon Health Sciences University/Oregon Graduate Institute, Beaverton, Oregon

Field Effect Studies of $CoxTi1-xO_2$ Thin Films

AS Posadas, J Yau, C Ahn, Yale University, New Haven, Connecticut

Elemental Analysis of Bulk Aerosol Samples Collected with Drum Impactor during MCMA 2003 Field Study

RS Disselkamp, Pacific Northwest National Laboratory, Richland, Washington

MJ Molina, BM Zuberi, KS Johnson, Massachusetts Institute of Technology, Cambridge, Massachusetts

A Laskin, Environmental Molecular Sciences Laboratory, Richland, Washington

Continuous Isosorbide Production

JE Holladay, Pacific Northwest National Laboratory, Richland, Washington

New Technologies for Reduction of Automobile Exhaust Emissions

CH Peden, H Zhao, Pacific Northwest National Laboratory, Richland, Washington

Bioavailability of Arsenic in Dislodgeable Residue from Pressure-Treated Wood

BM Sass, Battelle Columbus, Columbus, Ohio

XPS Characterization of Diesel Soot Materials

D Kim, Pacific Northwest National Laboratory, Richland, Washington

Characterization of Regenerable CO_2 Sorbents

F Zheng, Pacific Northwest National Laboratory, Richland, Washington

Europium Uptake in Various SAM Coated Mesoporous Silica

RS Addleman, ED Bott, Pacific Northwest National Laboratory, Richland, Washington

JT Bays, U.S. Military Academy, West Point, New York

TEM and XPS Analysis of Ligand-functionalized Semiconductor Quantum Dots used in Biodetection Studies

MG Warner, CJ Bruckner-Lea, Pacific Northwest National Laboratory, Richland, Washington

Phenotypic Characterization of TCE and PCE Degrading *Dehalococcoides*

MR Fisk, AR Sabalowsky, LC Semprini, LB Parker, NW Chambers, Oregon State University, Corvallis, Oregon

Investigation of Strain in InGaN MQW Structures

MC Johnson, Lawrence Berkeley National Laboratory, University of California, Berkeley, Berkeley, California

Oxidation of Lead Sulfide Surfaces in the Presence of Phosphate: Nanoparticle Formation

AG Stack, WH Casey, University of California, Davis, Davis, California

TEM and SEM Investigation of Non-pathogenic Bacterial Cultures

A Dohnalkova, Environmental Molecular Sciences Laboratory, Richland, Washington

Observations of Scytonema-colonized and Non-colonized Fiber Cement Roofing Shingles

RM Fisher, BA Reine, Lab/Cor, Inc., Seattle, Washington

Magnetic and Transport Studies of Co Doped TiO_2 Thin Films

A Punnoose, Boise State University, Boise, Idaho

Composition Characterization of ZnO:Cr and ZnO:Co

BK Roberts, K Krishnan, G Gardner, University of Washington, Seattle, Washington

MBE Growth of Epitaxial Anatase TiO_2 (001) on STO(001) on Si(001) and Characterization of TiO_2 Films

KA Griffin, K Krishnan, University of Washington, Seattle, Washington

Fabrication and Characterization of Functional Nanostructured Materials

S Jin, X Ye, University of California, San Diego, La Jolla, California

Synthesis and Characterization at Atomic Level of Novel Nanocrystalline Metal Oxide Structures

Z Yu, Nanjing Normal University, Nanjing, China

Surface Analysis of Metal Carbides

Y Shin, Pacific Northwest National Laboratory, Richland, Washington

Analysis of Catalysts and Microchannel Components

VS Stenkamp, KP Brooks, DL King, W Tegrotenhuis, CM Fischer, Pacific Northwest National Laboratory, Richland, Washington

STM Tip Analysis by TEM

Z Dohnalek, Pacific Northwest National Laboratory, Richland, Washington

Sulfur Absorbents for Emission Control

L Li, Pacific Northwest National Laboratory, Richland, Washington

Development of a Soldier-Portable Power System

DR Palo, Pacific Northwest National Laboratory, Richland, Washington

Characterization of Surface and Materials

C Lei, Pacific Northwest National Laboratory, Richland, Washington

SEM Characterization of Proposed Hydrogen Storage Materials

LE Thomas, Pacific Northwest National Laboratory, Richland, Washington

XPS Analysis of Fuel Cell Components

LR Pederson, GW Coffey, O Marina, Pacific Northwest National Laboratory, Richland, Washington

Investigation of Elemental Contamination in Solid Oxide Fuel Cell Materials

VL Sprenkle, Pacific Northwest National Laboratory, Richland, Washington

Investigation of the Stability of Secondary Precipitates Incorporated with Contaminants

W Um, Pacific Northwest National Laboratory, Richland, Washington

Analysis of Catalysts

D Elliott, Pacific Northwest National Laboratory, Richland, Washington

Chalcogenide Surface Science

BR Johnson, Pacific Northwest National Laboratory, Richland, Washington

MH Engelhard, Environmental Molecular Sciences Laboratory, Richland, Washington

Hydrogenation of Pyrolysis Oils to Create Gasoline

T Hart, D Elliott, Pacific Northwest National Laboratory, Richland, Washington

Characterization of Lithium Aluminate Powders

BR Johnson, T Hart, Pacific Northwest National Laboratory, Richland, Washington

Deposition of Metal-Doped Oxides for Spintronic Applications

TC Kaspar, SA Chambers, TC Droubay, Pacific Northwest National Laboratory, Richland, Washington

DE McCready, T Thevuthasan, V Shutthanandan, C Wang, AS Lea, Environmental Molecular Sciences Laboratory, Richland, Washington

Study of Compositional Variations in Combinatorially-sputtered Transparent Conductive Oxides

PE Burrows, DW Matson, Pacific Northwest National Laboratory, Richland, Washington

Probing Cation Disordering in $Gd_2Ti_2O_7$ Pyrochlore by X-ray Photoelectron Spectroscopy

RC Ewing, J Lian, University of Michigan, Ann Arbor, Michigan

***In situ* XPS Measurements of Reforming Catalysts**

En Fox, C Song, Pennsylvania State University, University Park, Pennsylvania

V Subramani, Research Triangle Institute, Research Triangle Park, North Carolina

Studies of Corrosion of Materials by Lead Alloys for Advanced Reactor and Nuclear Waste Amelioration Applications

AL Johnson, JW Farley, DJ Koury, DA Parsons, TT Ho, U Younas, University of Nevada, Las Vegas, Las Vegas, Nevada

EP Loewen, Idaho National Engineering and Energy Laboratory, Idaho Falls, Idaho

Influence of Gd and Sm Doping on Atomic and Ionic Transport Properties of Novel Nanostructured Ceria-Zirconia Multilayers

Y Wang, S Kuchibhatla, S Seal, University of Central Florida, Orlando, Florida

O Marina, DW Matson, J Gilmore, A Cinson, M Dyer, L Bauder, Pacific Northwest National Laboratory, Richland, Washington

AA El-Azab, Florida State University, Tallahassee, Florida

T Thevuthasan, L Saraf, C Wang, V Shutthanandan, P Nachimuthu, Environmental Molecular Sciences Laboratory, Richland, Washington

Z Yu, Nanjing Normal University, Nanjing, China

MV Stodola, National Electrostatics Corporation, Middleton, Wisconsin

Catalyst Characterization

RS Disselkamp, Pacific Northwest National Laboratory, Richland, Washington

Catalyst and Support Characterization

RS Disselkamp, Y Chin, Pacific Northwest National Laboratory, Richland, Washington

Catalyst and Support Characterization

RS Disselkamp, J Kwak, J Szanyi, Pacific Northwest National Laboratory, Richland, Washington

B Arey, Cn Wang, Environmental Molecular Sciences Laboratory, Richland, Washington

Formation of Silicides by Ion Beam Synthesis

CT Jonsson, Lund Institute of Technology, Lund University, Lund, Sweden

HJ Whitlow, University of Jyväskylä, University of Jyväskylä, Finland

Hydrogen Storage

T Autrey, Pacific Northwest National Laboratory, Richland, Washington

AM Feaver, University of Washington, Seattle, Washington

Fundamental Studies of Oxygen Storage Materials

CH Peden, J Szanyi, E Ozensoy, Pacific Northwest National Laboratory, Richland, Washington

C Yi, Texas A&M University, College Station, Texas

Fundamental Studies of NOx Adsorber Materials

J Kwak, CH Peden, J Szanyi, D Kim, RG Tonkyn, Xn Wang, D Tran, CM Verrier, J Fain, Pacific Northwest National Laboratory, Richland, Washington

Early Transition Metal Oxides as Catalysts: Crossing Scales from Clusters to Single Crystals to Functioning Materials - Catalysis Science

CH Peden, Y Wang, J Hu, J Herrera, Pacific Northwest National Laboratory, Richland, Washington

Nanotemplated Electrodeposition

DB Allred, DT Schwartz, University of Washington, Seattle, Washington

Conductivity of Functionalized Carbon Nanotube Films

R Khairoutdinov, University of Alaska, Fairbanks, Fairbanks, Alaska

Irradiation Induced 3-D Ordered Arrays of Nanostructure

L Wang, S Zhu, T Ding, University of Michigan, Ann Arbor, Michigan

Nanoengineered Electrochemical Sensors for Mixed Wastes

W Liao, Y Lin, University of Idaho, Moscow, Idaho

Y Lin, Z Wang, W Yantasee, J Wang, G Liu, JR Bontha, H Wu, SL Riechers, Pacific Northwest National Laboratory, Richland, Washington

A Lee, National University of Singapore, Singapore, Malaysia

X Cui, Fudan University, Shanghai, China

Develop Stable Bipolar Membranes

JR Bontha, Pacific Northwest National Laboratory, Richland, Washington

Characterization of Sputter Deposited Co Doped TiO_2 Films

KA Griffin, K Krishnan, University of Washington, Seattle, Washington

Hydrogen Storage of Chemical Hydrides

L Li, Pacific Northwest National Laboratory, Richland, Washington

Crystallization Behavior of Bulk Amorphous Alloy

A Bandyopadhyay, S Bose, Washington State University, Pullman, Washington

Kiln Phosphoric Acid

JA Megy, JDC, Inc, New Cumberland, West Virginia

Structural Characterization of Nanoporous Thin Films

Z Dohnalek, Pacific Northwest National Laboratory, Richland, Washington

Passive Film Stability in Alloy 22

S Seal, D Bera, University of Central Florida, Orlando, Florida

RH Jones, CF Windisch, Pacific Northwest National Laboratory, Richland, Washington

DR Baer, Environmental Molecular Sciences Laboratory, Richland, Washington

Measurements of Aerosol and Aerosol Precursors during the Summer 2004 Northeast Aerosol Experiment (NEAX)

PH Daum, Brookhaven National Laboratory, Upton, New York

Microcharacterization of Engineered Mono-Sodium Titanate

EC Buck, Pacific Northwest National Laboratory, Richland, Washington

Characterization of Nanostructured Ceramics

S Bose, Washington State University, Pullman, Washington

X-ray Photoelectron Spectroscopy of Materials for Hydrogen Storage

BJ Tarasevich, Pacific Northwest National Laboratory, Richland, Washington

Synthesis of Cu_2O under Protein Control

H Dai, DT Schwartz, University of Washington, Seattle, Washington

Deposition of Fuel Cell Materials

VL Sprenkle, CA Coyle, Pacific Northwest National Laboratory, Richland, Washington

Deposition of Fuel Cell Materials

VL Sprenkle, CA Coyle, ES Mast, Pacific Northwest National Laboratory, Richland, Washington

Yttrium Phosphate/Gadolinum Phosphate Particles for Cancer Imaging and Treatment

A Gutowska, Advanced Imaging Technologies, Richland, Washington

Microstructural Investigations of Novel Magnetic Oxide Semiconductors

A Punnoose, MR Kongara, Boise State University, Boise, Idaho

Catalysis Collaborative Access Team (CAT)

CH Peden, Pacific Northwest National Laboratory, Richland, Washington

M Chen, DW Goodman, P Han, Texas A&M University, University Park, Pennsylvania

RJ Chimentao, University of Washington, Seattle, Washington

JM White, University of Texas at Austin, Austin, Texas

Atmospheric Emissions Collaborative Access Team (CAT)

JM Hales, Envair, Pasco, Washington

Controlled Defect Generation in Porous Silicon

Z Wang, Pacific Northwest National Laboratory, Richland, Washington

DR Baer, Environmental Molecular Sciences Laboratory, Richland, Washington

FS Ou, State University of New York at Buffalo(SUNY), Geneseo, New York

ATM, ISO and Other Standard and Metrology Measurements for Surface Analysis

DR Baer, Environmental Molecular Sciences Laboratory, Richland, Washington

R Wallace, University of Texas at Dallas, Richardson, Texas

Ion Channeling Studies of Epitaxial Oxide Films and Gas-Solid Interfaces

KR Padmanabhan, Wayne State University, Detroit, Michigan

Soft Lithography for Optics

G Dunham, JC Birnbaum, CR Batishko, JA Willett, Pacific Northwest National Laboratory, Richland, Washington

Nanomaterial Toxicology

DR Baer, Environmental Molecular Sciences Laboratory, Richland, Washington

Aging of Lean NOX Traps

BG Bunting, Oak Ridge National Laboratory, Knoxville, Tennessee

Characterization of Cr(III) Solid Phases

D Rai, Pacific Northwest National Laboratory, Richland, Washington

Surface Cleanliness of Si Wafer after Laser Treatment

L Scudiero, Washington State University, Pullman, Washington

XPS Studies of Coablt Phthalocyanine Thin Films

KW Hipps, WA English, Washington State University, Pullman, Washington

Surface Characterization of Calcium Phosphates

WJ Shaw, Pacific Northwest National Laboratory, Richland, Washington

B Arey, Environmental Molecular Sciences Laboratory, Richland, Washington

Origin of the Face Dependent Photocatalytic Activity of TiO_2:Probing Surface Chemistry with Molecular Adsorption

U Diebold, TJ Beck, A Klust, Tulane University, New Orleans, Louisiana

MA Henderson, Pacific Northwest National Laboratory, Richland, Washington

Photochemical Studies on N-doped TiO_2 Single Crystals - Fundamental Investigations of Water Splitting on Model TiO_2 (Mike Henderson's BES Project - 48526)

VH Lam, University of Central Florida, Orlando, Florida

MA Henderson, SA Chambers, S Cheung, R Shao, SC Andrews, Pacific Northwest National Laboratory, Richland, Washington

IV Lyubinetsky, T Thevuthasan, P Nachimuthu, Environmental Molecular Sciences Laboratory, Richland, Washington

EK Vestergaard, University of Washington, Seattle, Washington

MD Robbins, JM White, University of Texas at Austin, Austin, Texas

Size Selected Gas-phase Soot Aerosol Oxidation

SH Kim, National Institute of Standards and Technology, Gaithersburg, Maryland

MR Zachariah, University of Maryland, Gaithersburg, Maryland

SEM Image of Microparticles

RM Ozanich, Pacific Northwest National Laboratory, Richland, Washington

XPS Analysis on Tungten Oxide Nanoclusters Supported on MCM41.

J Herrera, Pacific Northwest National Laboratory, Richland, Washington

Chrome Volatility

GD Maupin, Pacific Northwest National Laboratory, Richland, Washington

TW Wietsma, Environmental Molecular Sciences Laboratory, Richland, Washington

Structure and Property Tailoring of Metal Nanoparticles Dispersed in Dielectrics by High Energy Ion Implantation

L Ream, Pacific Northwest National Laboratory, Richland, Washington

G Duscher, North Carolina State University, Raleigh, North Carolina

C Wang, V Shutthanandan, T Thevuthasan, B Arey, Environmental Molecular Sciences Laboratory, Richland, Washington

New Materials as Sulfur Absorbents

L Li, Pacific Northwest National Laboratory, Richland, Washington

Surface Analysis of IAQ VOC Sensors

M Kleefstra, AirAdvice Inc., Portland, Oregon

The Characterization of Aluminum Nitride-silicon Carbide Alloy Crystals on Silicon Carbide Substrates

JH Edgar, Z Gu, Kansas State University, Manhattan, Kansas

Surface State Characterization of Pt/Al_2O_3 Catalyst for the CPO Reaction

KL Hohn, C Cao, Kansas State University, Manhattan, Kansas

Gas Cell Metalization

KC Antolick, JI McIntyre, G Dunham, Pacific Northwest National Laboratory, Richland, Washington

Chemical Analysis of Nano-structures for Toxic Gas Detection

DW Galipeau, South Dakota State University, Brookings, South Dakota

Synthesis and Characterization of Enzyme Nanoparticles

G Liu, Pacific Northwest National Laboratory, Richland, Washington

Mesopore Uniformity and Hydrothermal Stability of Silica Thin Films for High Permeabilty Applications

S Li, A Qiao, Pacific Northwest National Laboratory, Richland, Washington

B Arey, Environmental Molecular Sciences Laboratory, Richland, Washington

Determination of Pore Structure in Highly Porous Silica Oxide Powders

LS Fifield, RD Champion, Pacific Northwest National Laboratory, Richland, Washington

Characterization of Corrosion Products on Iron Aluminide Coated Alloys

DJ Senor, Pacific Northwest National Laboratory, Richland, Washington

Surface Assessment of BxCy Thin Film on Si

AJ Carman, Pacific Northwest National Laboratory, Richland, Washington

XPS Investigations of Transition Metal Doped Oxide Semiconductors

J Hays, A Punnoose, Boise State University, Boise, Idaho

Effects of Ice-Clearing Chemicals

EV Stephens, Pacific Northwest National Laboratory, Richland, Washington

Testing of Carbon Based Materials for Hydrogen Storage

AM Feaver, G Cao, University of Washington, Seattle, Washington

Staff

S. Thevuthasan, Staff Scientist, Technical Lead
(509) 376-1375, theva@pnl.gov

Bruce W. Arey, Technologist
(509)376-3363, bruce.arey@pnl.gov

Barbara L. Diehl, Administrator
(509) 376-1518, barb@pnl.gov

Alice Dohnalkova, Senior Research Scientist
(509)376-3908, alice.donalkova@pnl.gov

Mark H. Engelhard, Research Scientist
(509) 376-1664, mark.engelhard@pnl.gov

A. Scott Lea, Senior Research Scientist
(509) 376-9145, scott.lea@pnl.gov

Igor V. Lyubinetsky, Senior Research Scientist
(509) 376-5220, igor.lyubinetsky@pnl.gov

David E. McCready, Research Scientist
(509) 376-9648, david.mccready@pnl.gov

P. Nachimuhtu, Senior Research Scientist
(509)276-1833, ponnusamy.nachimuthu@pnl.gov

Laxmikant V. Saraf, Senior Research Scientist
(509) 376-2006, laxmikant.saraf@pnl.gov

V. Shutthanandan, Senior Research Scientist
(509) 376-2708, shuttha@pnl.gov

Chongmin Wang, Senior Research Scientist
(509) 376-4292, chongmin.wang@pnl.gov

Yanwen Zhang, Senior Research Scientist
(509)376-3429, yanwen.zhang@pnl.gov

Zihua Zhu, Research Scientist
(509)376-2467, zihua.zhu@pnl.gov

We would also like to acknowledge the contributions from Gregory J. Exarhos, Charles H.F. Peden, Donald R. Baer, Jay W. Grate, Scott A. Chambers, William J. Weber, Michael A. Henderson, Michael J. White, Janos Szanyi, Do Heui Kim, Timothy C. Droubay,

Weilin Jiang, Mark E. Gross, Yong Wang, Yuehe Lin, Timothy L. Hubler, Todd R. Hart, Jungbae Kim, Jianli (John) Hu, Ja Hun Kwak and Robert S. Disselkamp.